INFERING NEUTRON STARS CRUST PROPERTIES

Deborah N. Aguilera

German Aerospace Center (DLR), Germany
CNEA-CAC, Buenos Aires, Argentina

with A.Turlione (PhD student) and J.Pons

arXiv: 1309.3909

- Motivation
- Five sources & open issues
- Theoretical approach
- Envelope models
- "Crustal coolers"
- Beyond crustal cooling --> (?)
- Conclusions

LMXB

Quiescent state --> little accretion $L_x \sim 10^{34}$ erg/s

Active phase --> accretion rises $L_x \sim 10^{36-39}$ erg/s

LMXB

Quiescent state --> little accretion $L_x \sim 10^{34}$ erg/s

Active phase --> accretion rises $L_x \sim 10^{36-39}$ erg/s

compression/heating of the envelope

thermonuclear fussion

Type I X-Ray Bursts

LMXB

Quiescent state --> little accretion $L_x \sim 10^{34}$ erg/s

Active phase --> accretion rises $L_x \sim 10^{36-39}$ erg/s

compression/heating of the envelope

thermonuclear fussion

Type I X-Ray Bursts

Quasi-persistent sources (accretion ~ 1-10 yrs)

Quiescent state --> little accretion $L_x \sim 10^{34}$ erg/s

Active phase --> accretion rises $L_x \sim 10^{36-39}$ erg/s

compression/heating of the envelope	compression/heating of the CRUST
thermonuclear fussion Type I X-Ray Bursts	pycnonuclear reacctions e-captures, n-emission

Quasi-persistent sources (accretion ~ 1-10 yrs)

Quiescent state --> little accretion Lx ~ 10^{34} erg/s

Active phase --> accretion rises Lx ~ 10^{36-39} erg/s

compression/heating of the envelope

thermonuclear fussion
Type I X-Ray Bursts

compression/heating of the CRUST

pycnonuclear reacctions
e-captures, n-emission

Quasi-persistent sources (accretion ~ 1-10 yrs)

Accretion stops --> X-ray quiescent emission
--> CRUSTAL COOLING

Brown et al (98, 09), Colpi et al (01), Rutledge (02), Shternin et al (07)

NSs going into quiescence

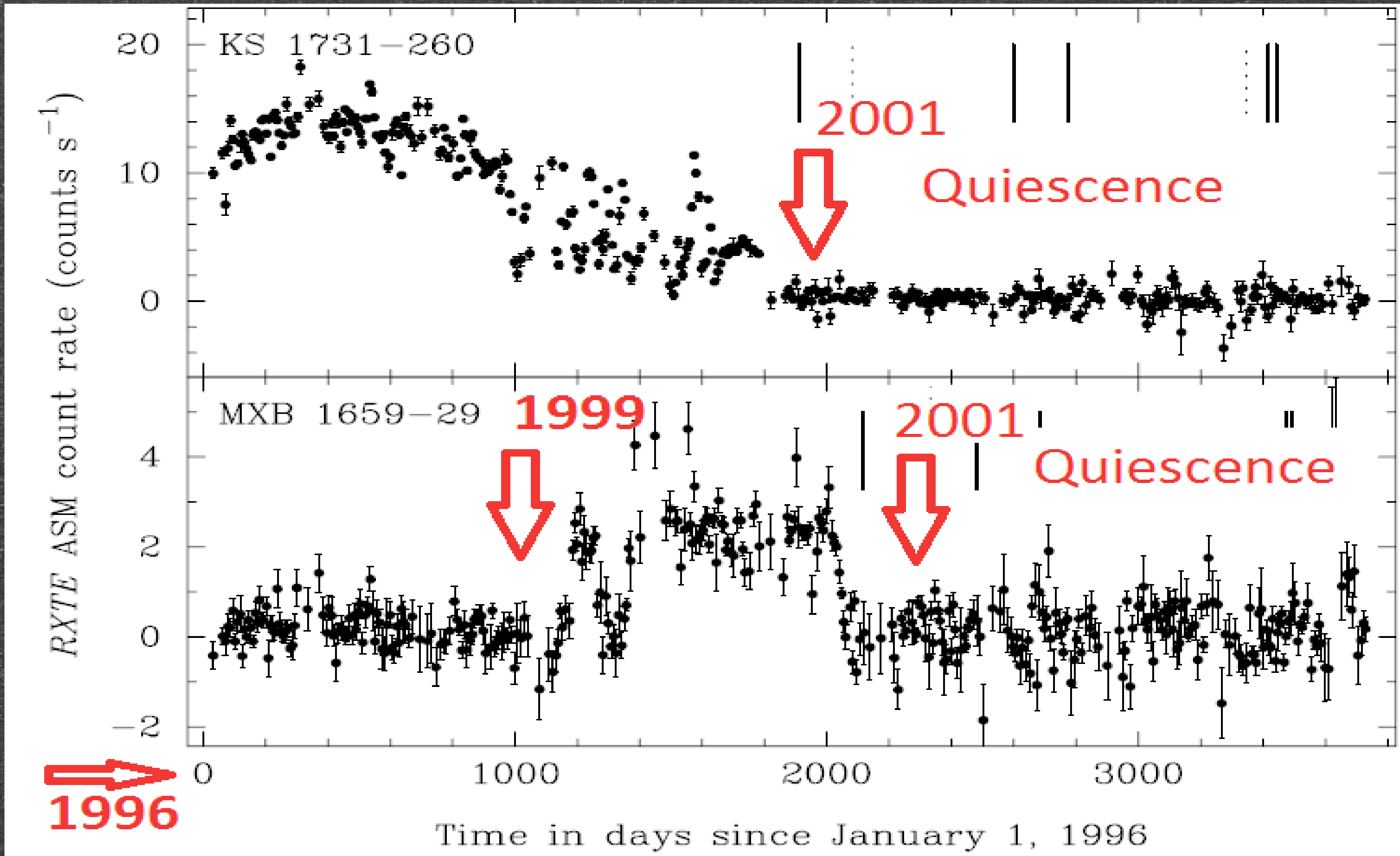

Cacket et al (2006)

Five sources detected

Source	$\dot{M}_{\rm obs}$ (10^{18}g s^{-1})	$t_{\rm acc}$ (yr)
MXB 1659−29[a]	0.07-0.18	2.5
KS 1731−260[b]	0.05-0.3	12.5
EXO 0748−676 *Chandra* [c] *Swift*[d] *XMM-Newton* [d] *all data*[d]	0.03	24
XTE J1701−462[e]	1.1	1.6
IGR J17480−2446[f]	0.2	0.17

Five sources detected

Source	$\dot{M}_{\rm obs}$ (10^{18}g s^{-1})	$t_{\rm acc}$ (yr)
MXB 1659−29[a]	0.07-0.18	2.5
KS 1731−260[b]	0.05-0.3	12.5
EXO 0748−676	0.03	24
Chandra [c]		
Swift[d]		
XMM-Newton [d]		
all data[d]		
XTE J1701−462[e]	1.1	1.6
IGR J17480−2446[f]	0.2	0.17

Five sources detected

Source	$\dot{M}_{obs}$ (10^{18} g s^{-1})	t_{acc} (yr)
MXB 1659−29[a]	0.07-0.18	2.5
KS 1731−260[b]		
EXO 0748−676		
Chandra [c]		
Swift[d]		
XMM-Newton [d]		
all data[d]		
XTE J1701−462[e]		
IGR J17480−2446[f]		

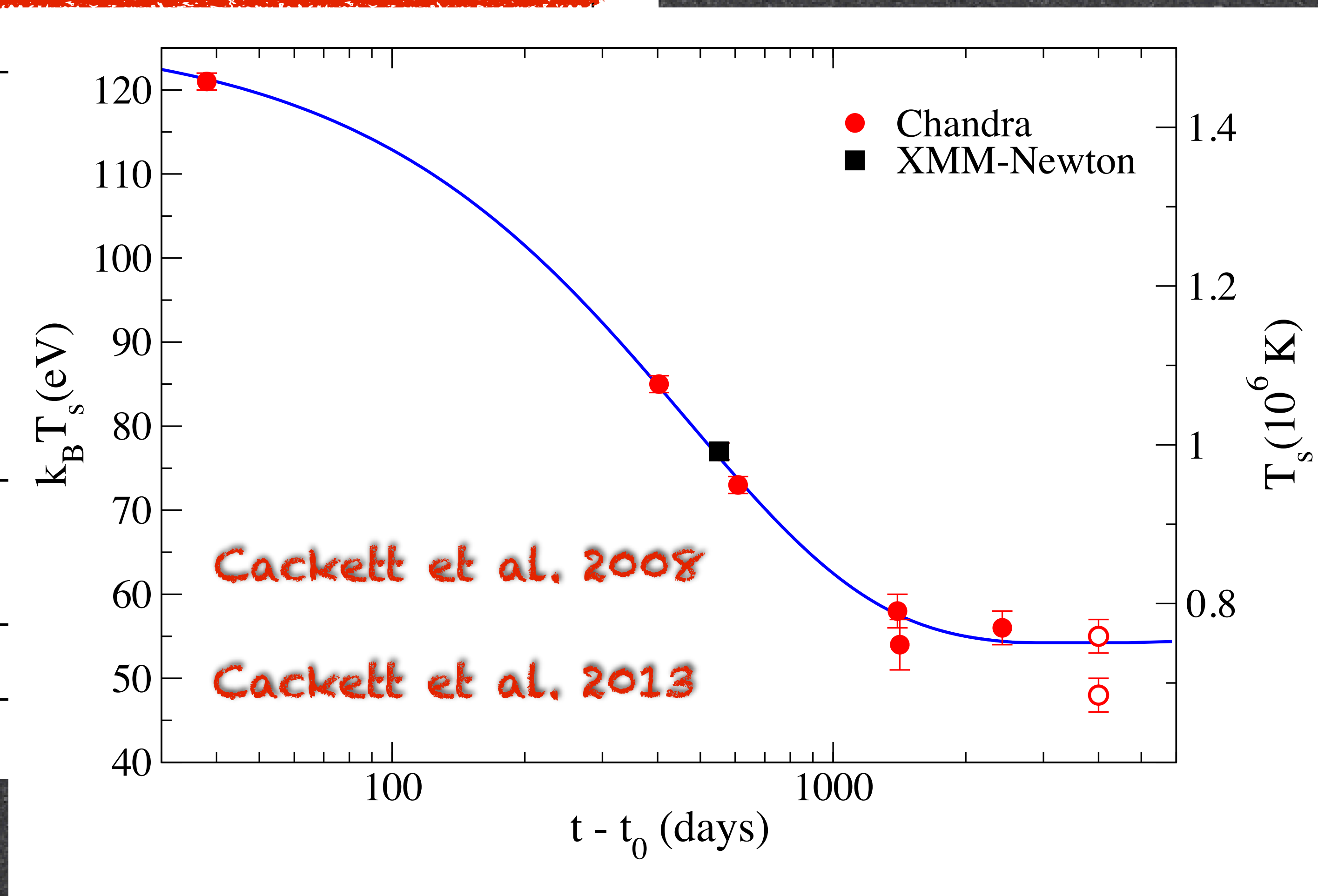

Five sources detected

Source	$\dot{M}_{\rm obs}$ (10^{18}g s^{-1})	$t_{\rm acc}$ (yr)
MXB 1659−29[a]	0.07-0.18	2.5
KS 1731−260[b]	0.05-0.3	12.5
EXO 0748−676	0.03	24
Chandra [c]		
Swift[d]		
XMM-Newton [d]		
all data[d]		
XTE J1701−462[e]	1.1	1.6
IGR J17480−2446[f]	0.2	0.17

Five sources detected

Source	$\dot{M}_{obs}$ (10^{18}g s^{-1})	t_{acc} (yr)
MXB 1659−29[a]	0.07-0.18	2.5
KS 1731−260[b]	0.05-0.3	12.5
EXO 0748−676		
Chandra [c]		
Swift[d]		
XMM-Newton [d]		
all data[d]		
XTE J1701−462[e]		
IGR J17480−2446[f]		

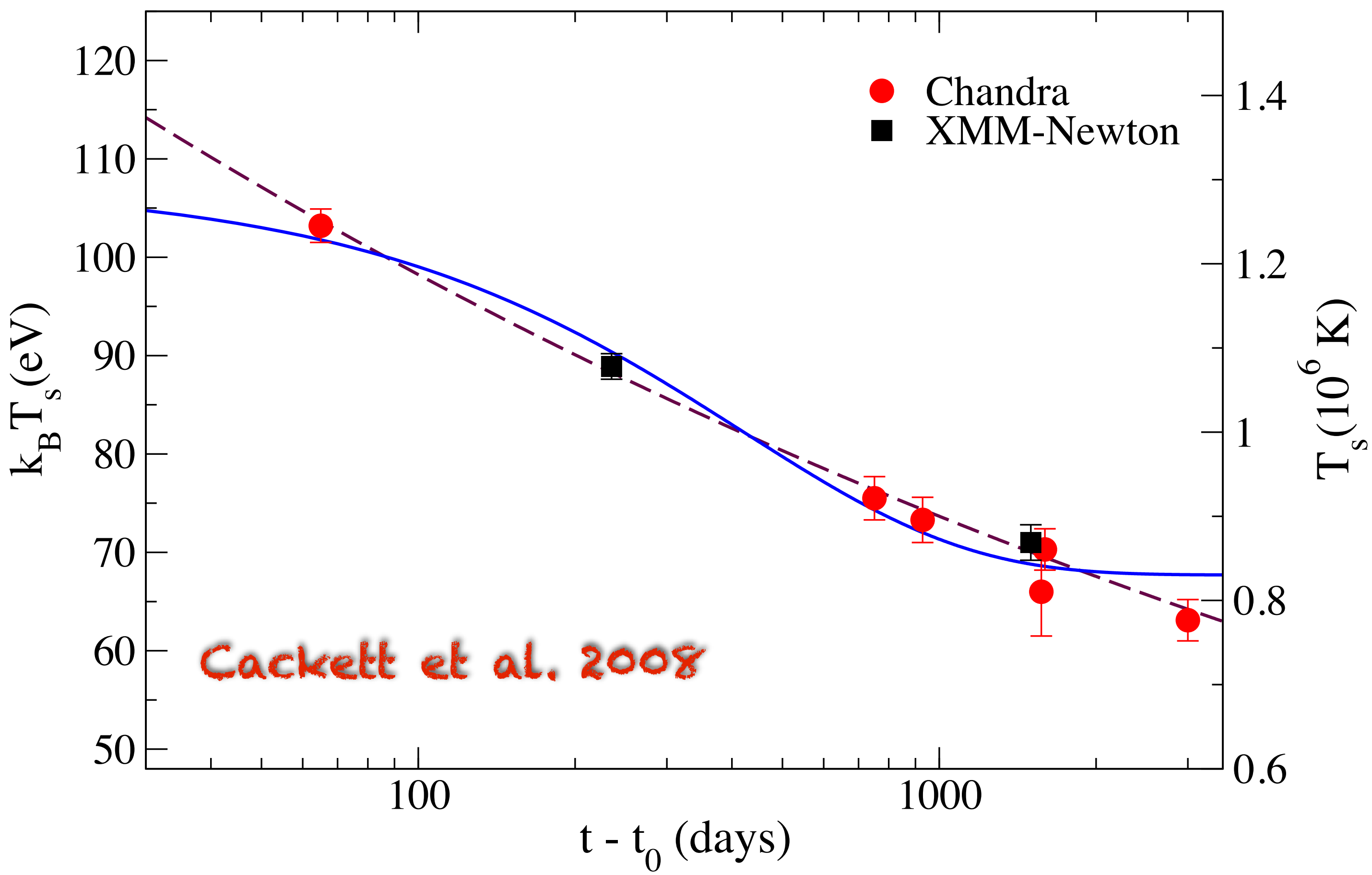

Five sources detected

Source	$\dot{M}_{\rm obs}$ (10^{18}g s^{-1})	$t_{\rm acc}$ (yr)
MXB 1659−29[a]	0.07-0.18	2.5
KS 1731−260[b]	0.05-0.3	12.5
EXO 0748−676 *Chandra* [c] *Swift*[d] *XMM-Newton* [d] *all data*[d]	0.03	24
XTE J1701−462[e]	1.1	1.6
IGR J17480−2446[f]	0.2	0.17

Five sources detected

Source	$\dot{M}_{\rm obs}$ (10^{18}g s^{-1})	$t_{\rm acc}$ (yr)
MXB 1659−29[a]	0.07-0.18	2.5
KS 1731−260[b]	0.05-0.3	12.5
EXO 0748−676	0.03	24
Chandra [c]		
Swift[d]		
XMM-Newton [d]		
all data[d]		
XTE J1701−462[e]		
IGR J17480−2446[f]		

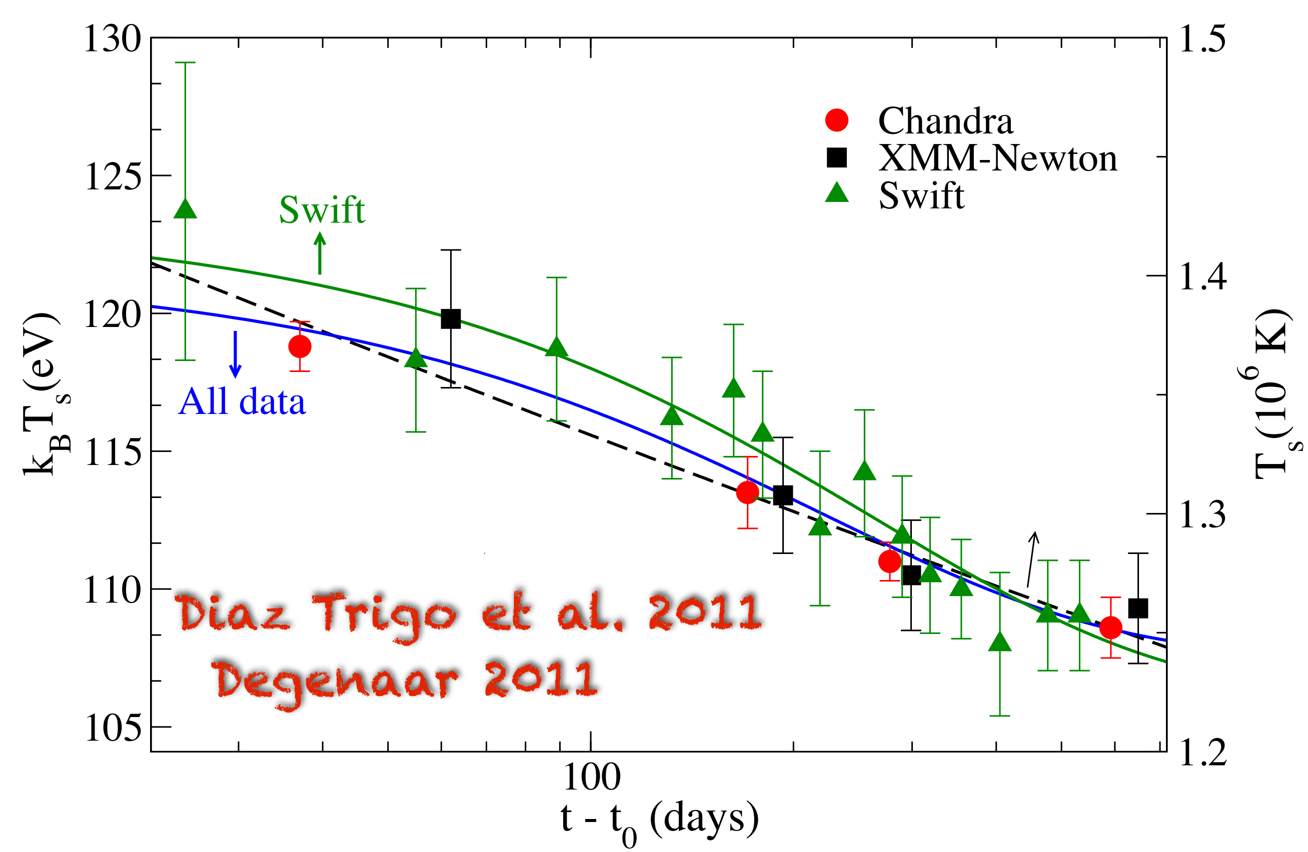

Five sources detected

Source	$\dot{M}_{\rm obs}$ (10^{18}g s^{-1})	$t_{\rm acc}$ (yr)
MXB 1659−29[a]	0.07-0.18	2.5
KS 1731−260[b]	0.05-0.3	12.5
EXO 0748−676	0.03	24
Chandra [c]		
Swift[d]		
XMM-Newton [d]		
all data[d]		
XTE J1701−462[e]	1.1	1.6
IGR J17480−2446[f]	0.2	0.17

Five sou

Source		
MXB 1659−29[a]		
KS 1731−260[b]		
EXO 0748−676		
Chandra [c]		
Swift[d]		
XMM-Newton [d]		
all data[d]		
XTE J1701−462[e]	1.1	1.6
IGR J17480−2446[f]	0.2	0.17

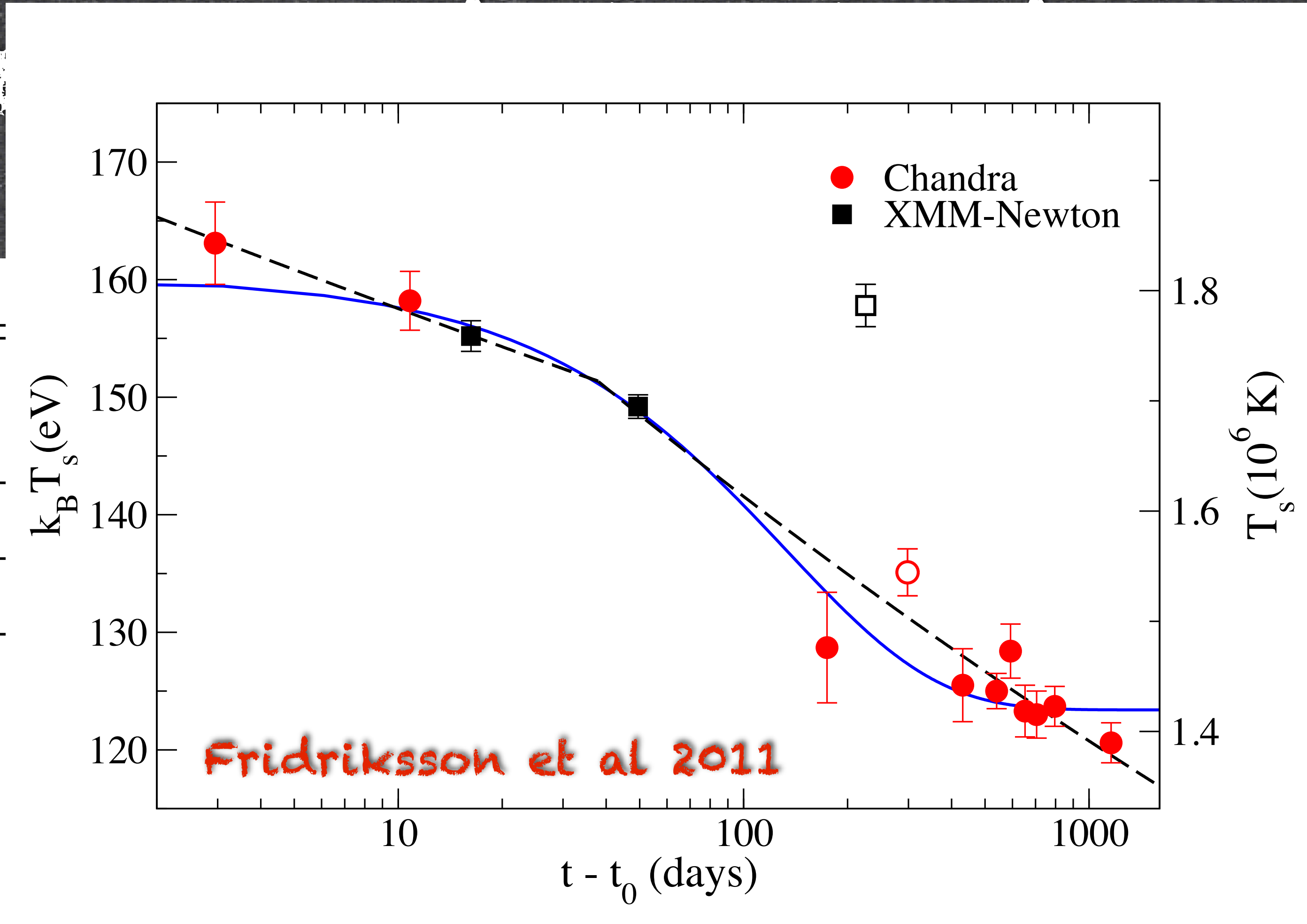

Five sources detected

Source	$\dot{M}_{\rm obs}$ (10^{18}g s^{-1})	$t_{\rm acc}$ (yr)
MXB 1659−29[a]	0.07-0.18	2.5
KS 1731−260[b]	0.05-0.3	12.5
EXO 0748−676 *Chandra* [c] *Swift*[d] *XMM-Newton* [d] *all data*[d]	0.03	24
XTE J1701−462[e]	1.1	1.6
IGR J17480−2446[f]	0.2	0.17

Five sources detected

Source		
MXB 1659−29[a]		
KS 1731−260[b]		
EXO 0748−676		
Chandra [c]		
Swift[d]		
XMM-Newton [d]		
all data[d]		
XTE J1701−462[e]	1.1	1.6
IGR J17480−2446[f]	0.2	0.17

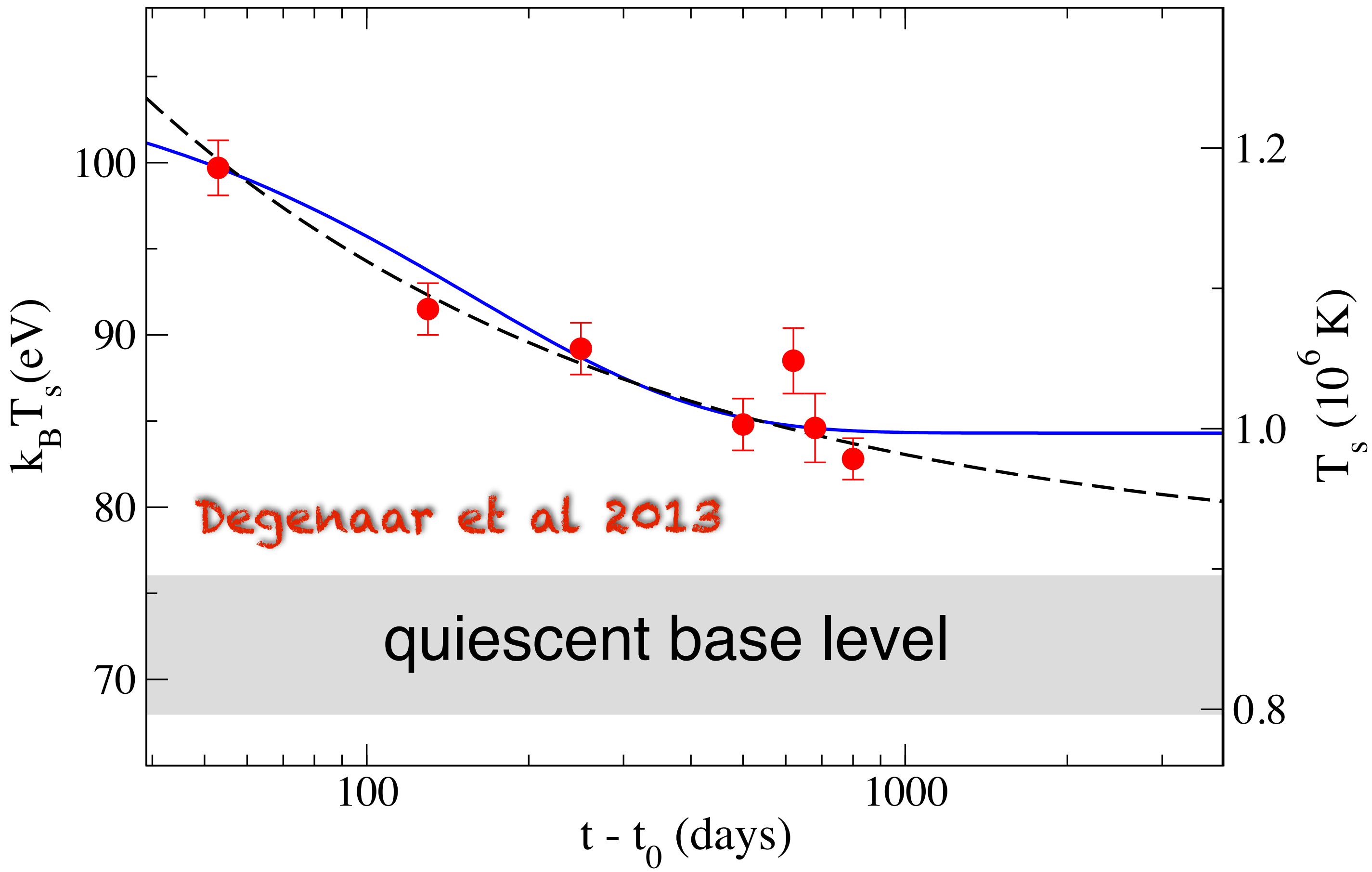

Modeling the crust thermal evolution

Modeling the crust thermal evolution

Heat sources

$$Q_{\dot{\mathrm{m}}} = \dot{m} \int_{\rho_s}^{\rho} q(\rho) d\rho = \dot{m} \sum_j q(\rho_j)$$

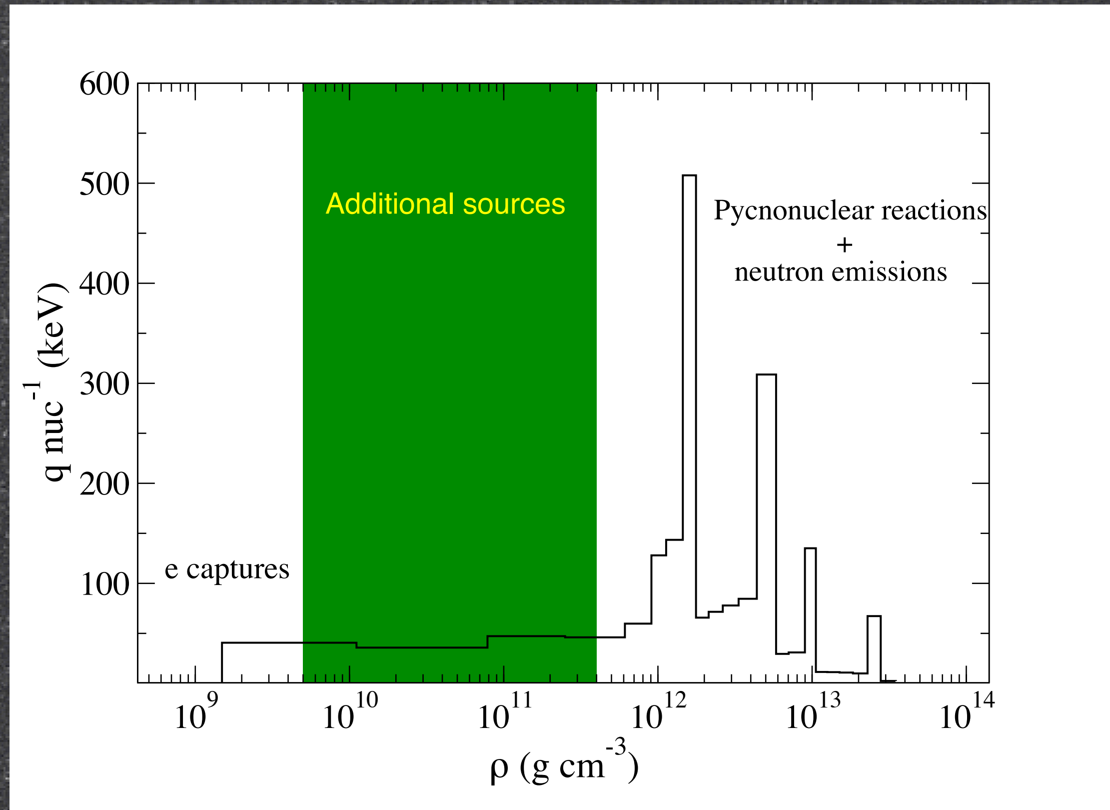

Modeling the crust thermal evolution

Heat sources

$$Q_{\dot{\rm m}} = \dot{m}\int_{\rho_s}^{\rho} q(\rho)d\rho = \dot{m}\sum_j q(\rho_j)$$

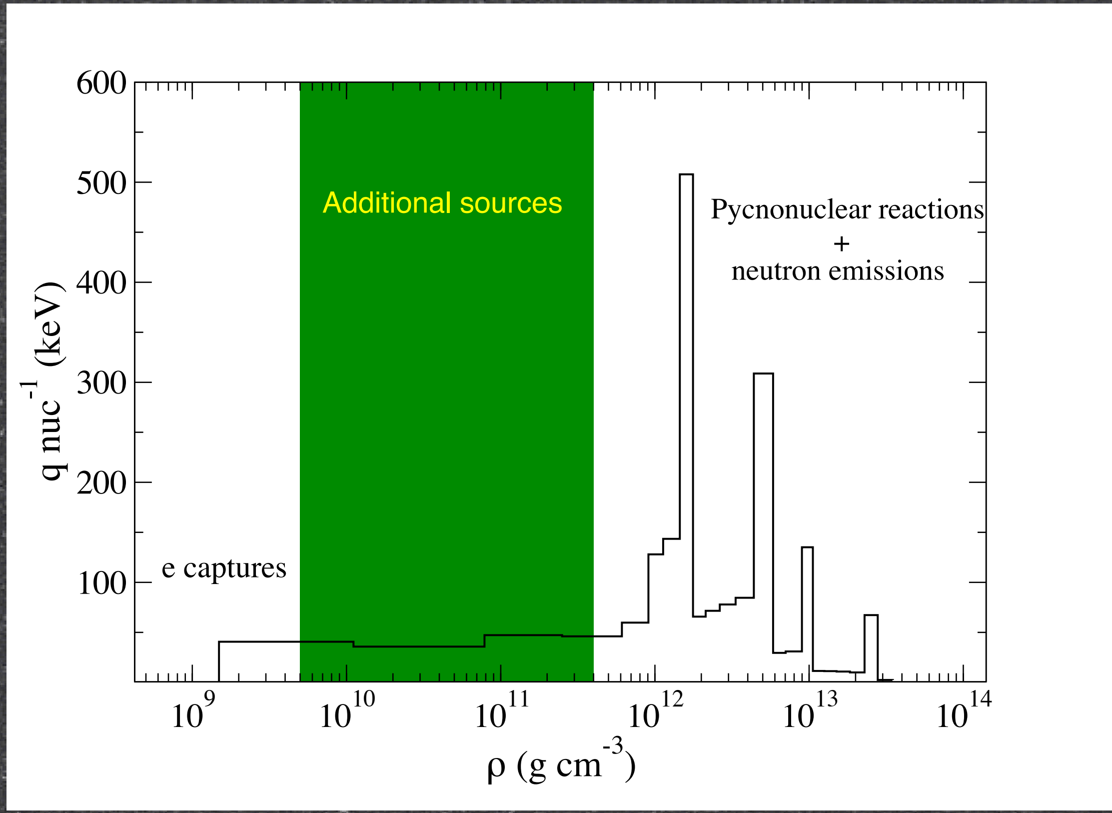

Diffusion equation

$$c_{\rm v}\frac{\partial T}{\partial t} = -\nabla\cdot F + Q_\nu + Q_{\dot{m}},$$

NS model includes: realistic accreted EoS, neutrino emissivity, specific heat, thermal conductivity, etc.

Modeling the crust thermal evolution

Heat sources

$$Q_{\dot{m}} = \dot{m} \int_{\rho_s}^{\rho} q(\rho) d\rho = \dot{m} \sum_j q(\rho_j)$$

Diffusion equation

$$c_{\rm v} \frac{\partial T}{\partial t} = -\nabla \cdot F + Q_\nu + Q_{\dot{m}},$$

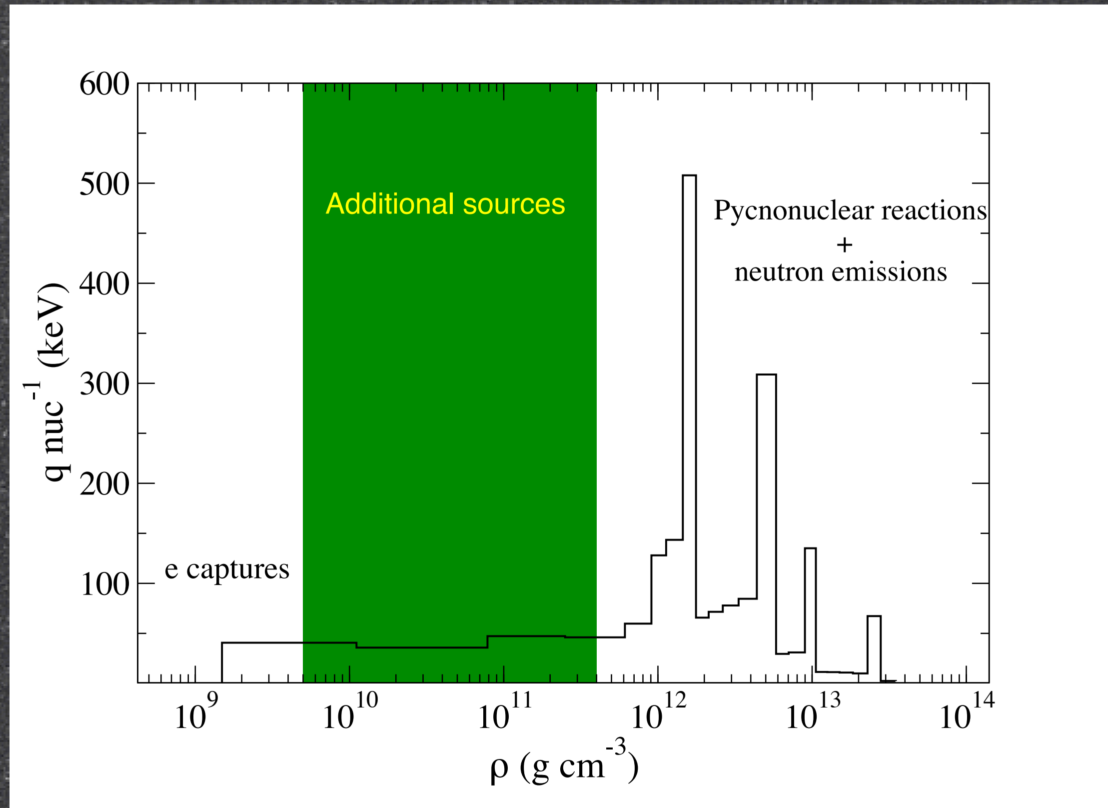

NS model includes: realistic accreted EoS, neutrino emissivity, specific heat, thermal conductivity, etc.

BC $\begin{cases} \text{inner T\_core constant} \\ \text{outer T\_envelope??} \end{cases}$

MXB 1659-29: Textbook crustal cooler

Initial thermal profile

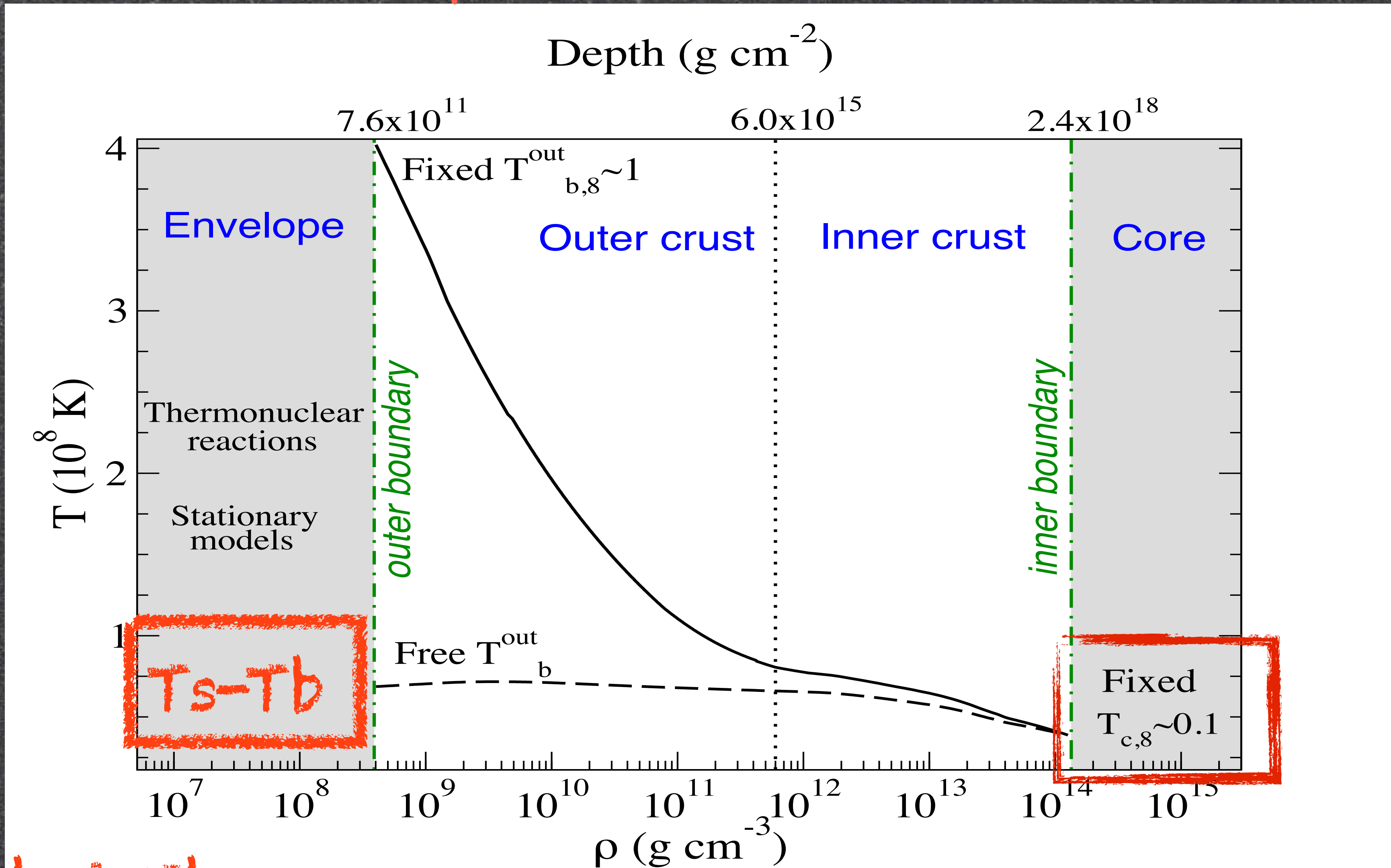

but Tb ???

MXB 1659-29: Textbook crustal cooler

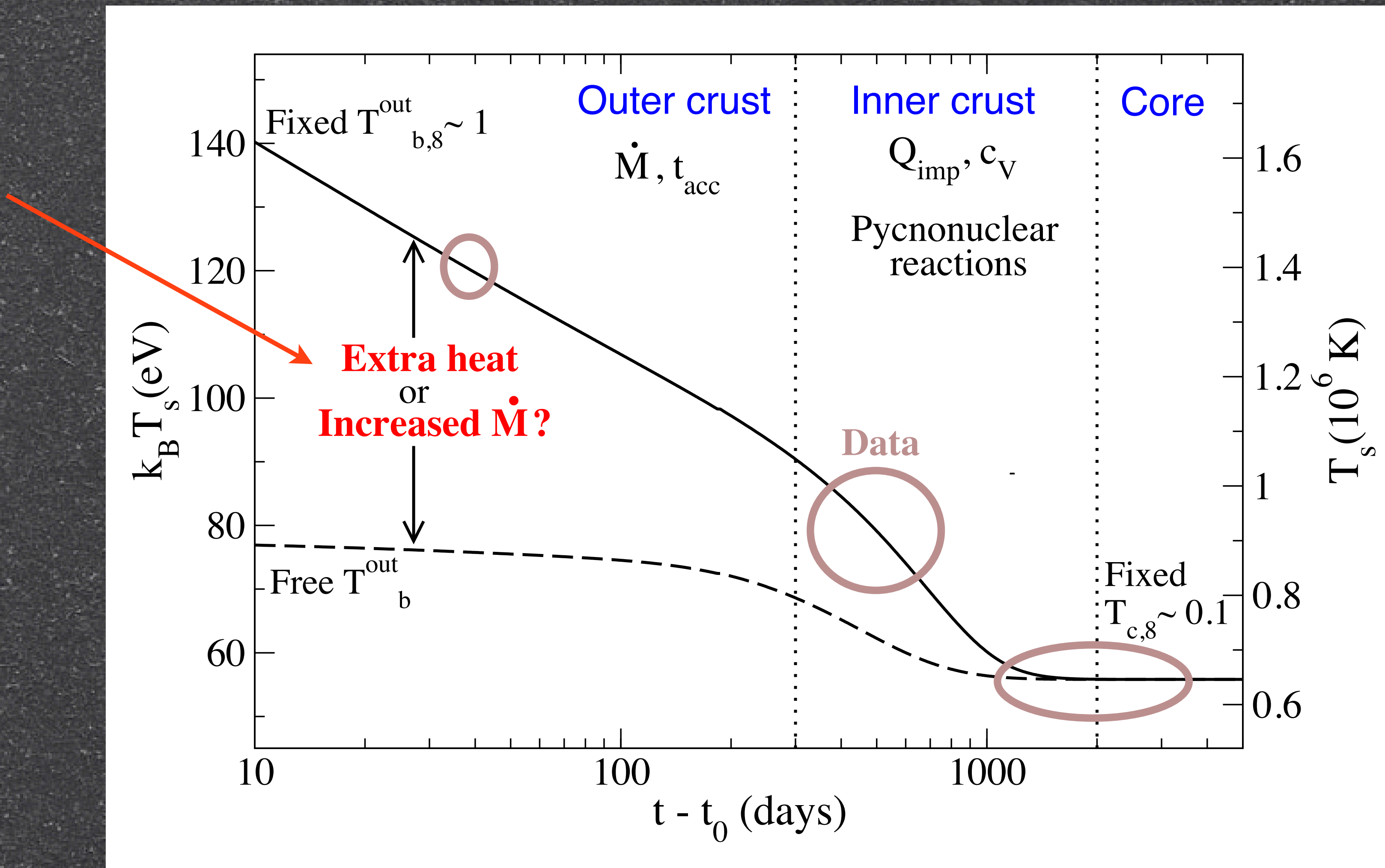

MXB 1659-29: Textbook crustal cooler

$T_b(\dot{M})$

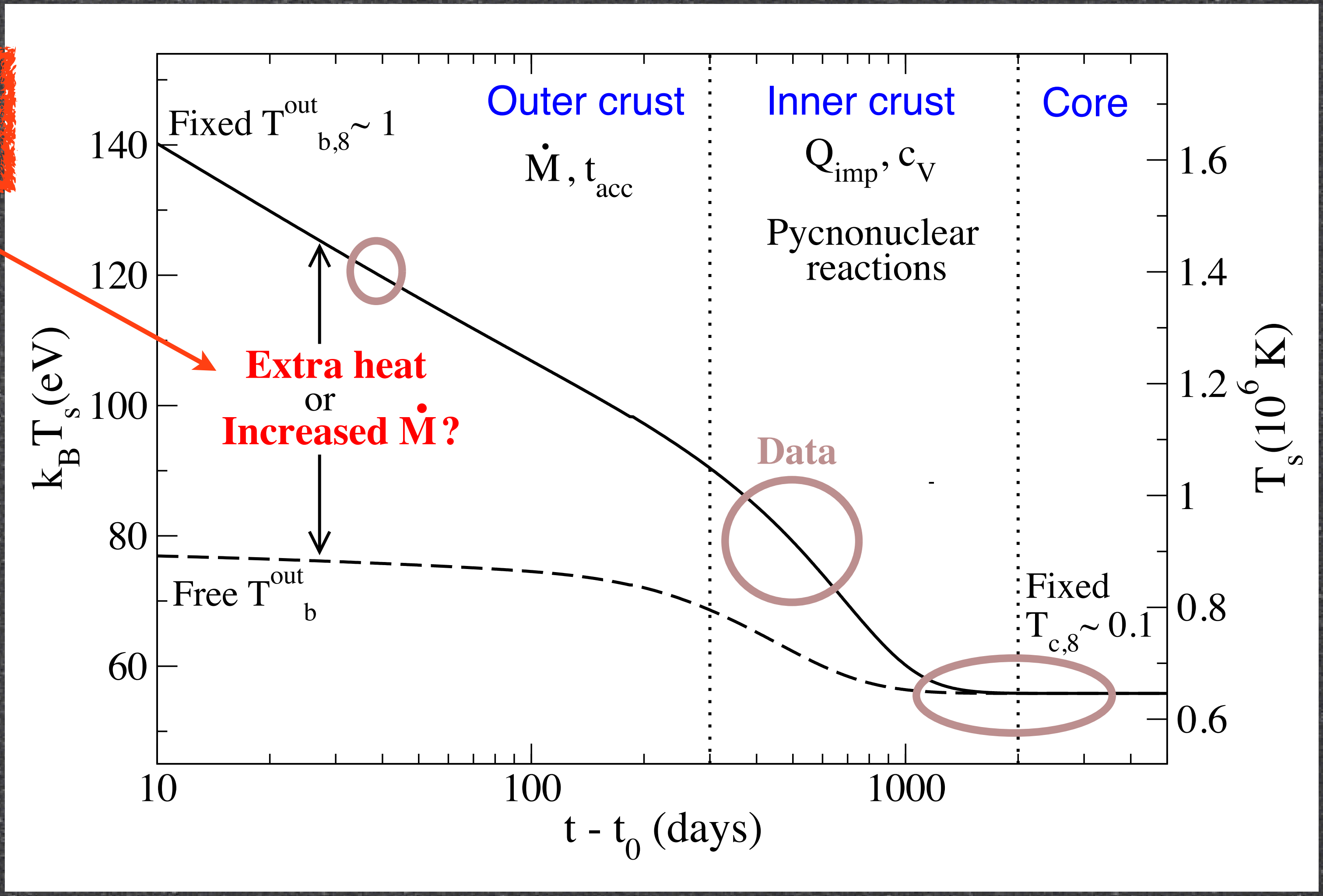

The envelope

in quiescence

in accretion

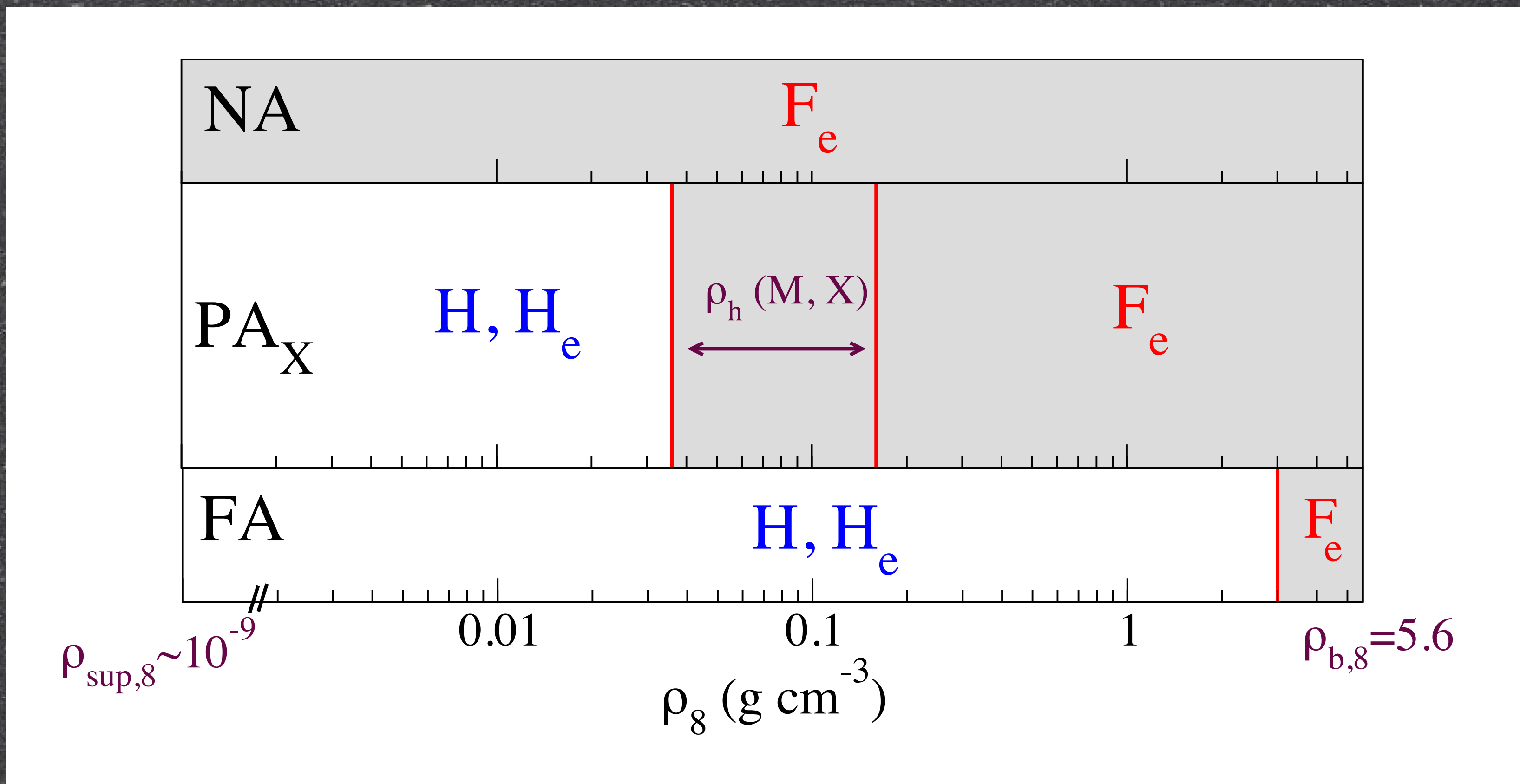

The envelope

in quiescence

in accretion

The envelope

in quiescence

in accretion

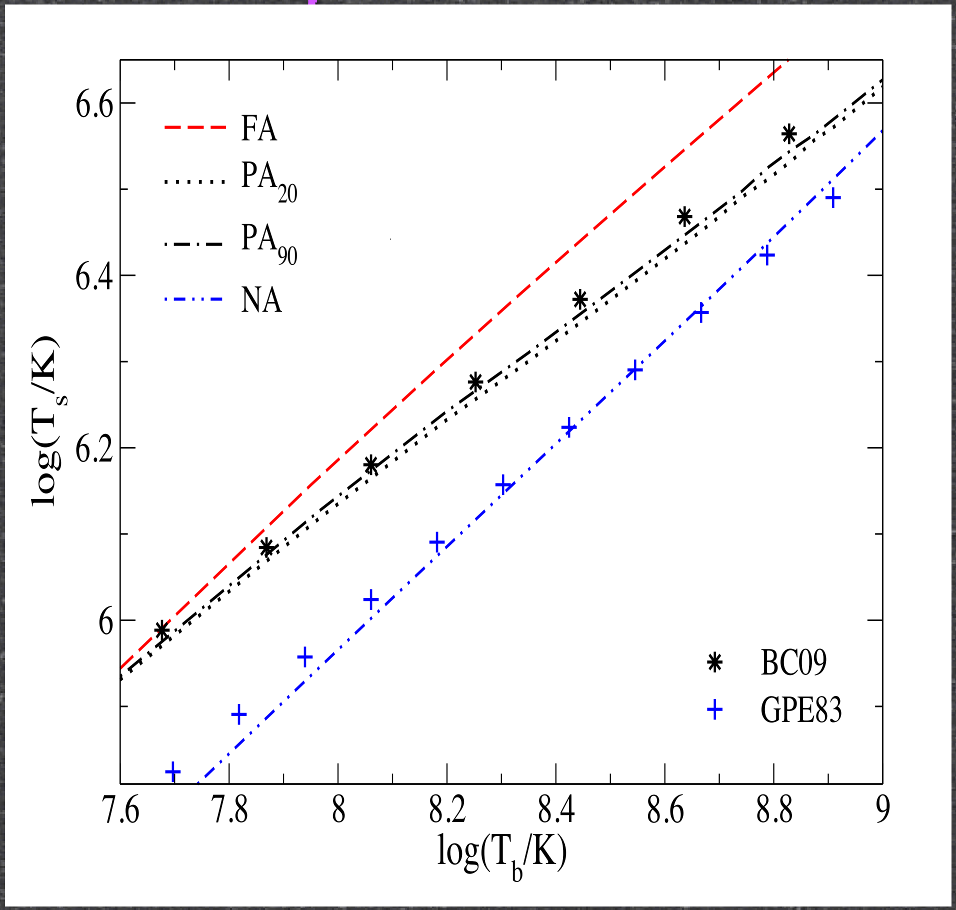

stationary solutions

The envelope

in quiescence

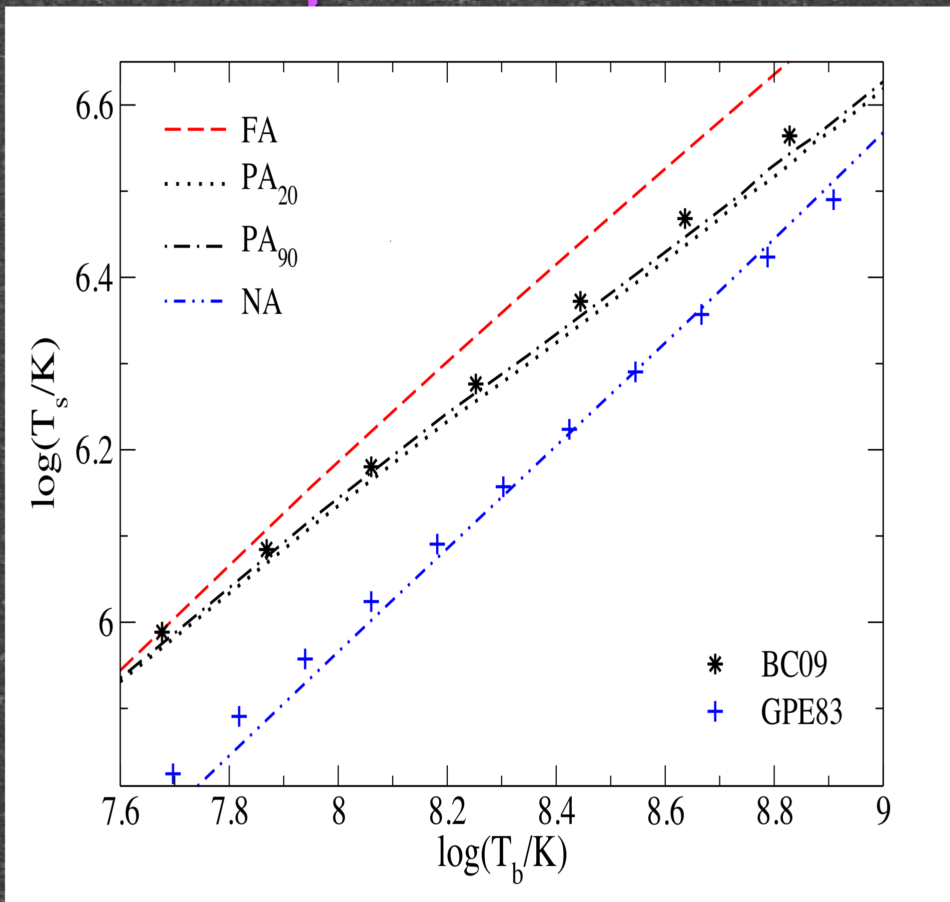

stationary solutions

in accretion

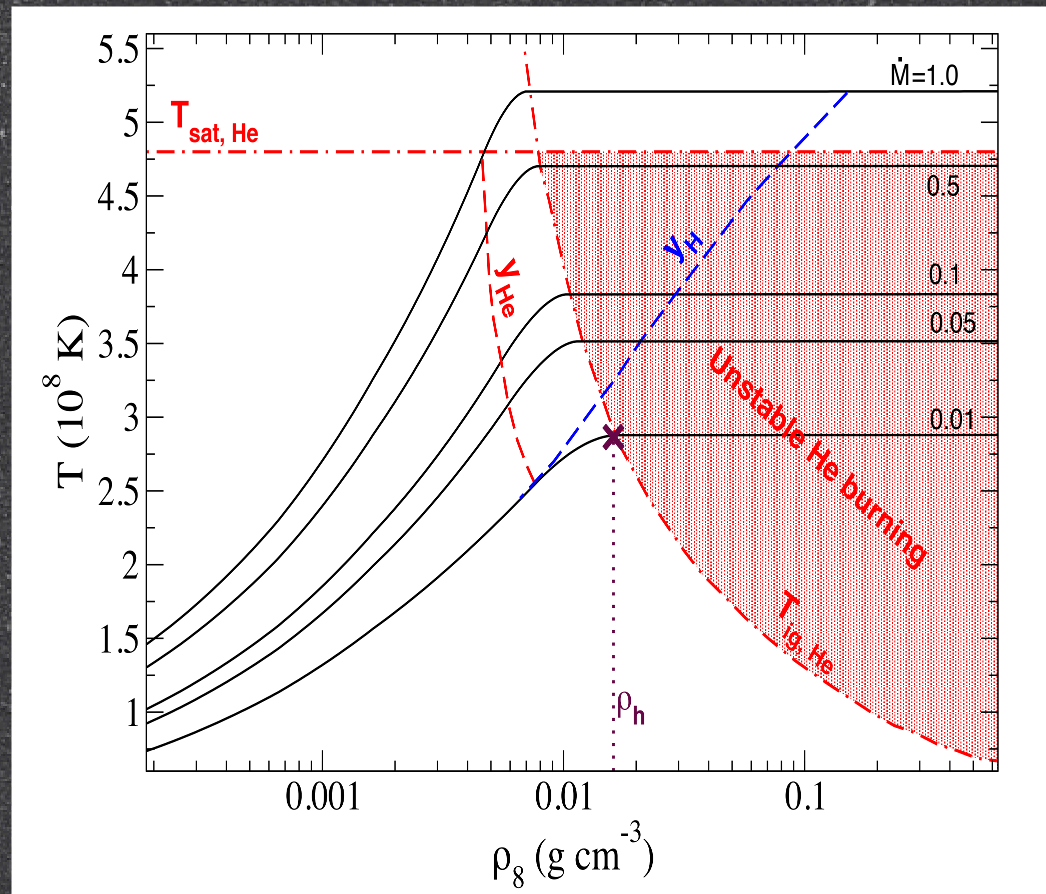

including hot CNO-cycle and 3-alpha generation rates

Bildsten (97)

Relations Tb (Ṁ)

Tb is modified in the active phase through Ṁ

--> stationary profiles for Tb(Ṁ)

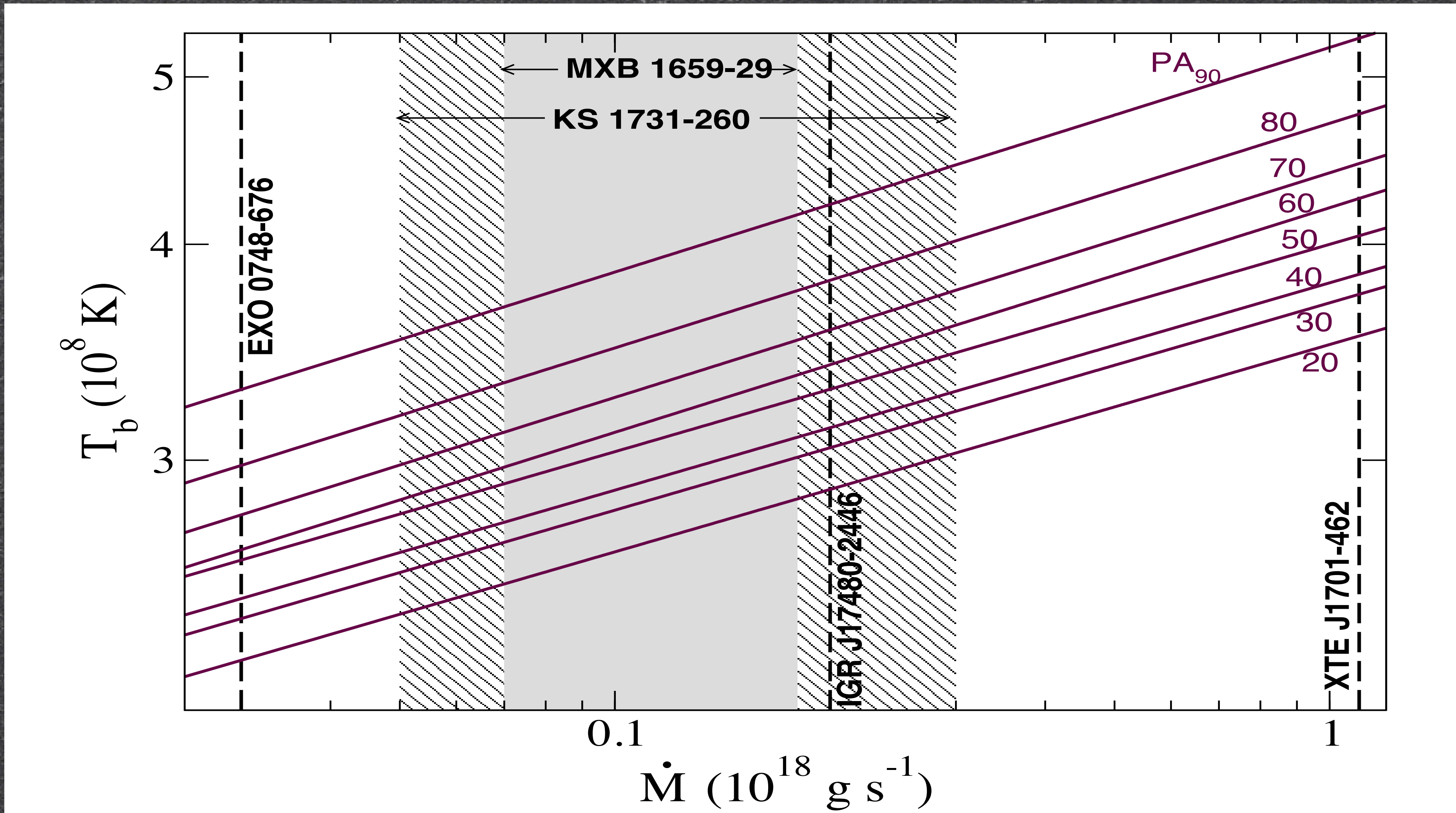

"Crustal coolers"

MXB 1659-29: Textbook crustal cooler

$\boxed{T_b(\dot{M})}$ → Reduces the # of free parameters

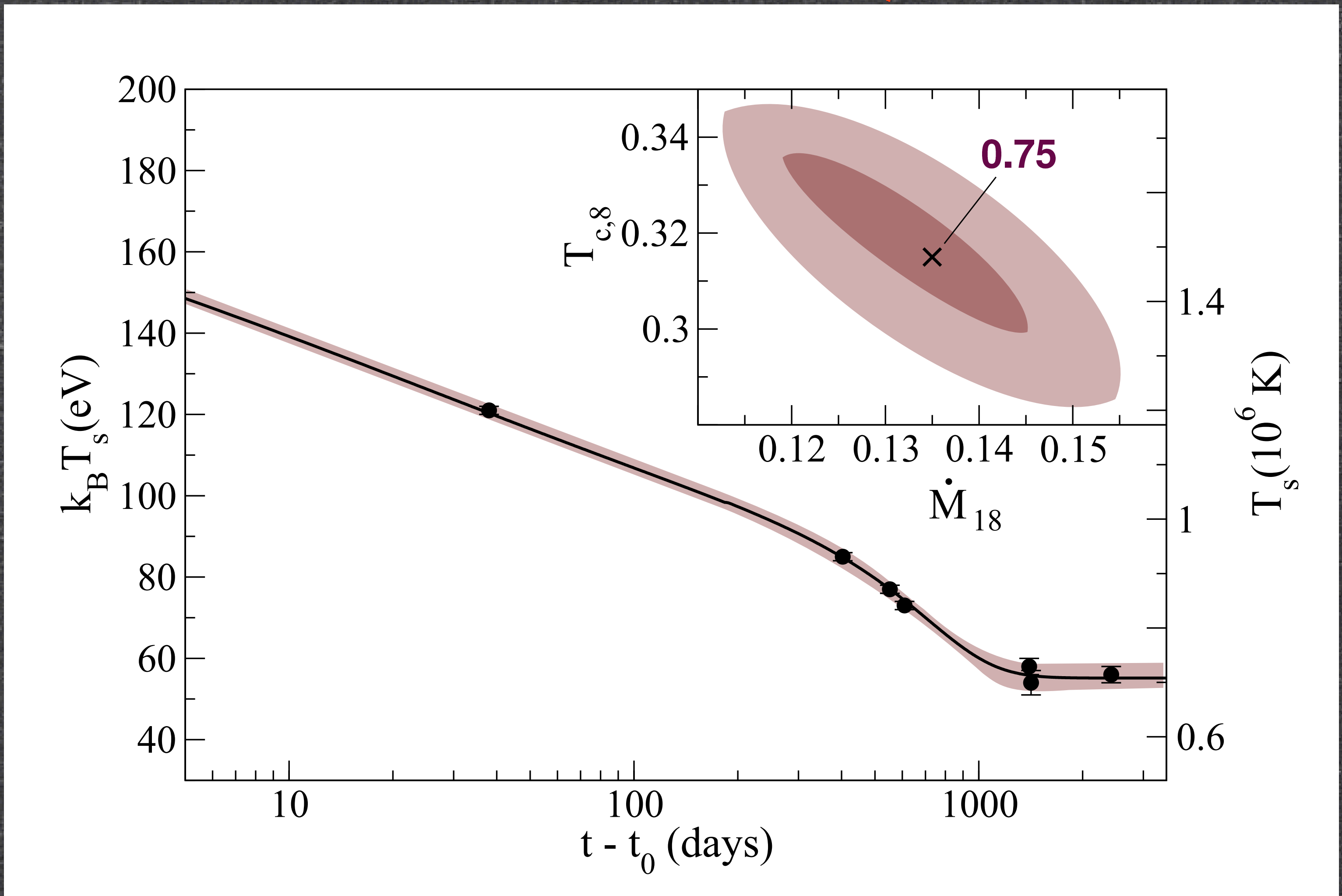

EXO 0748-676:
Hot crustal cooler

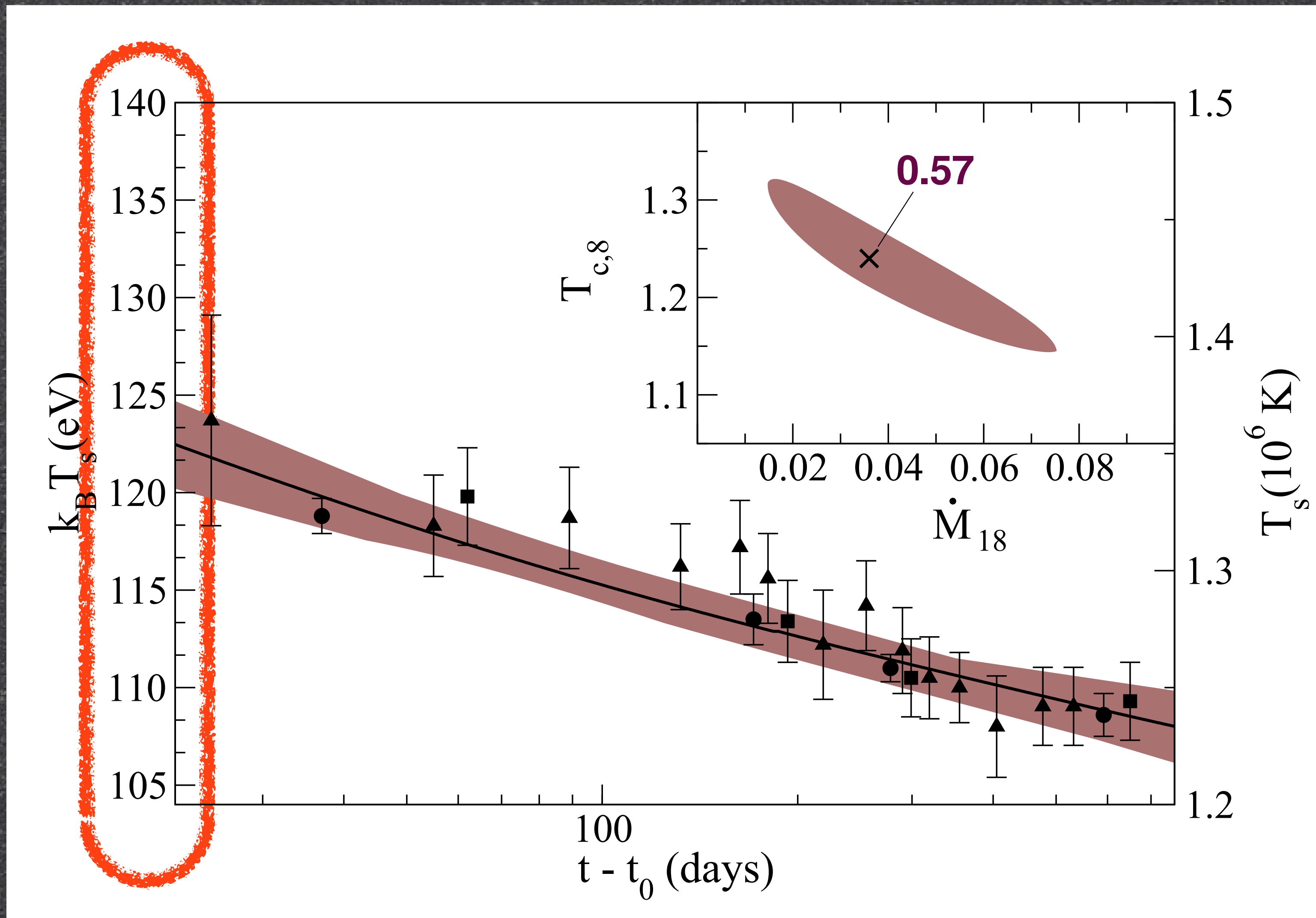

But....KS 1731-260 still cooling?

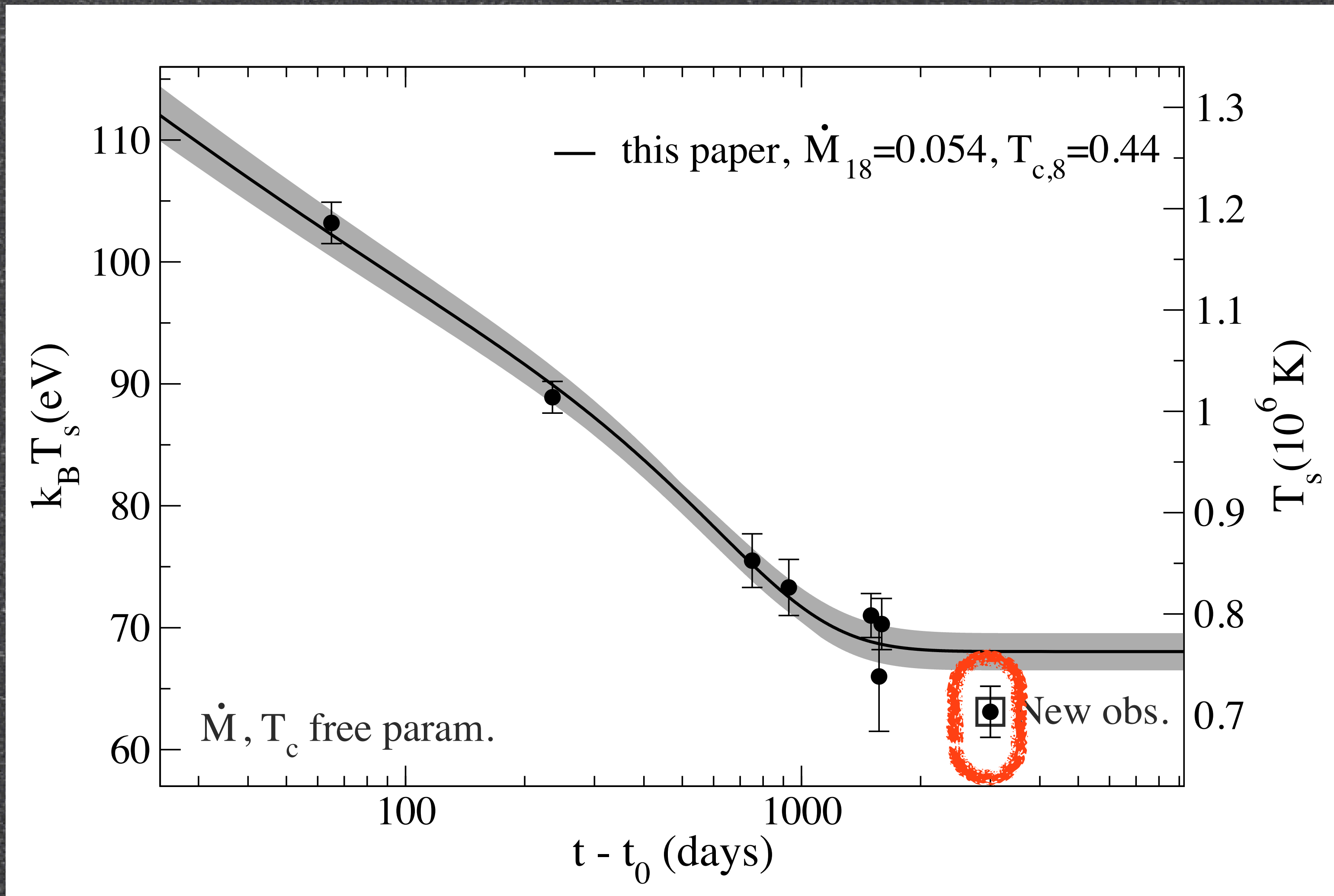

KS 1731-260 .... adjusting model

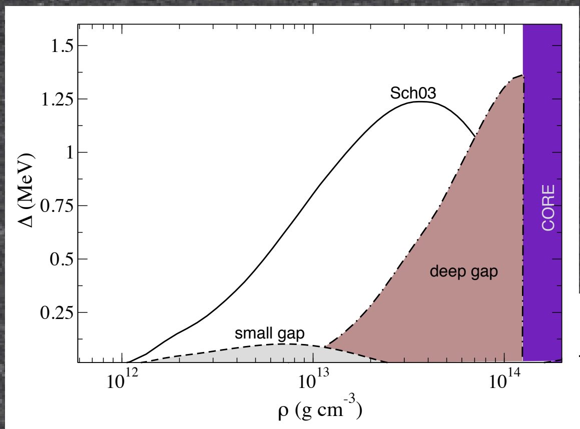

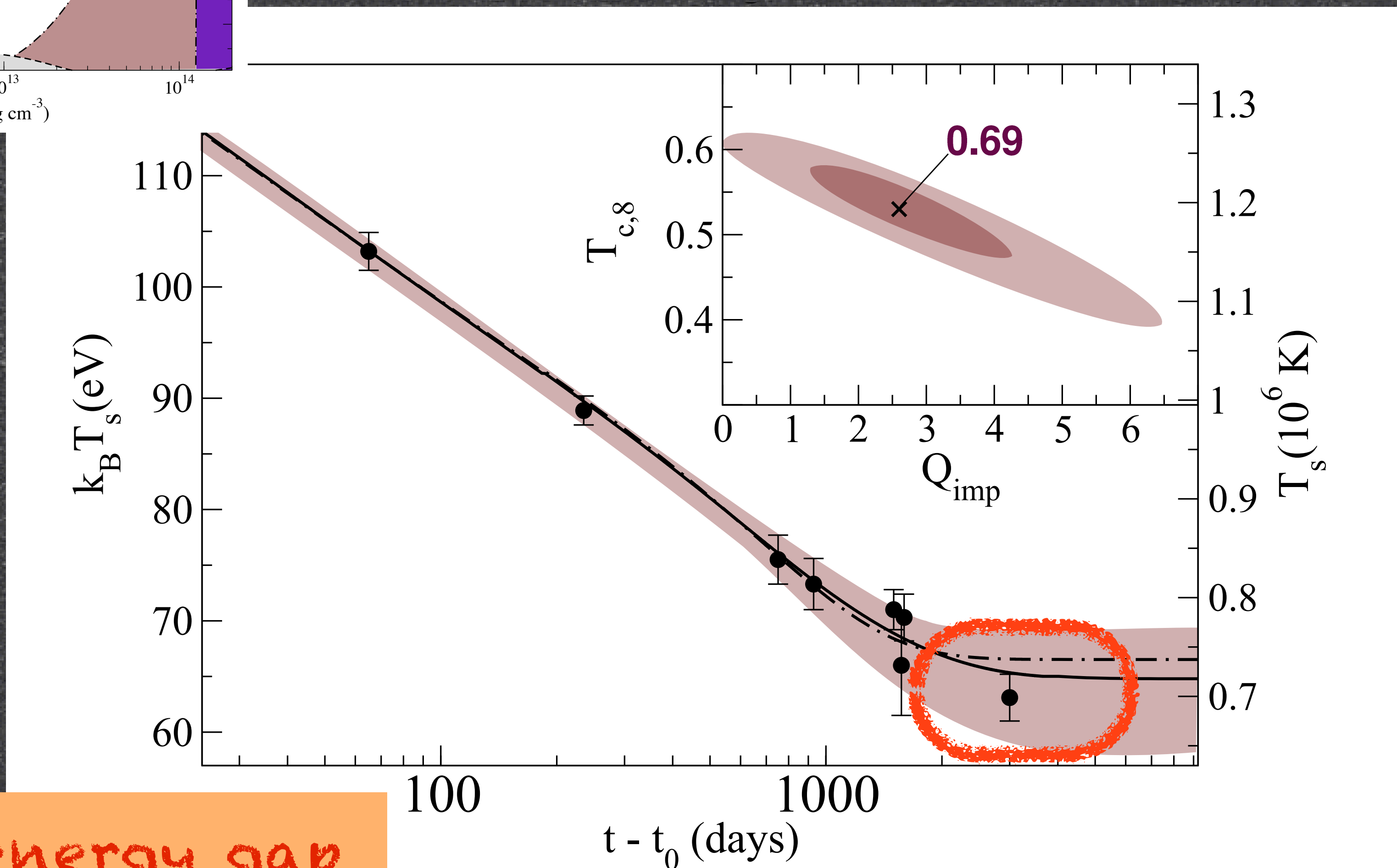

"deep" energy gap
for neutron SF!!

Constraints to crust/envelope

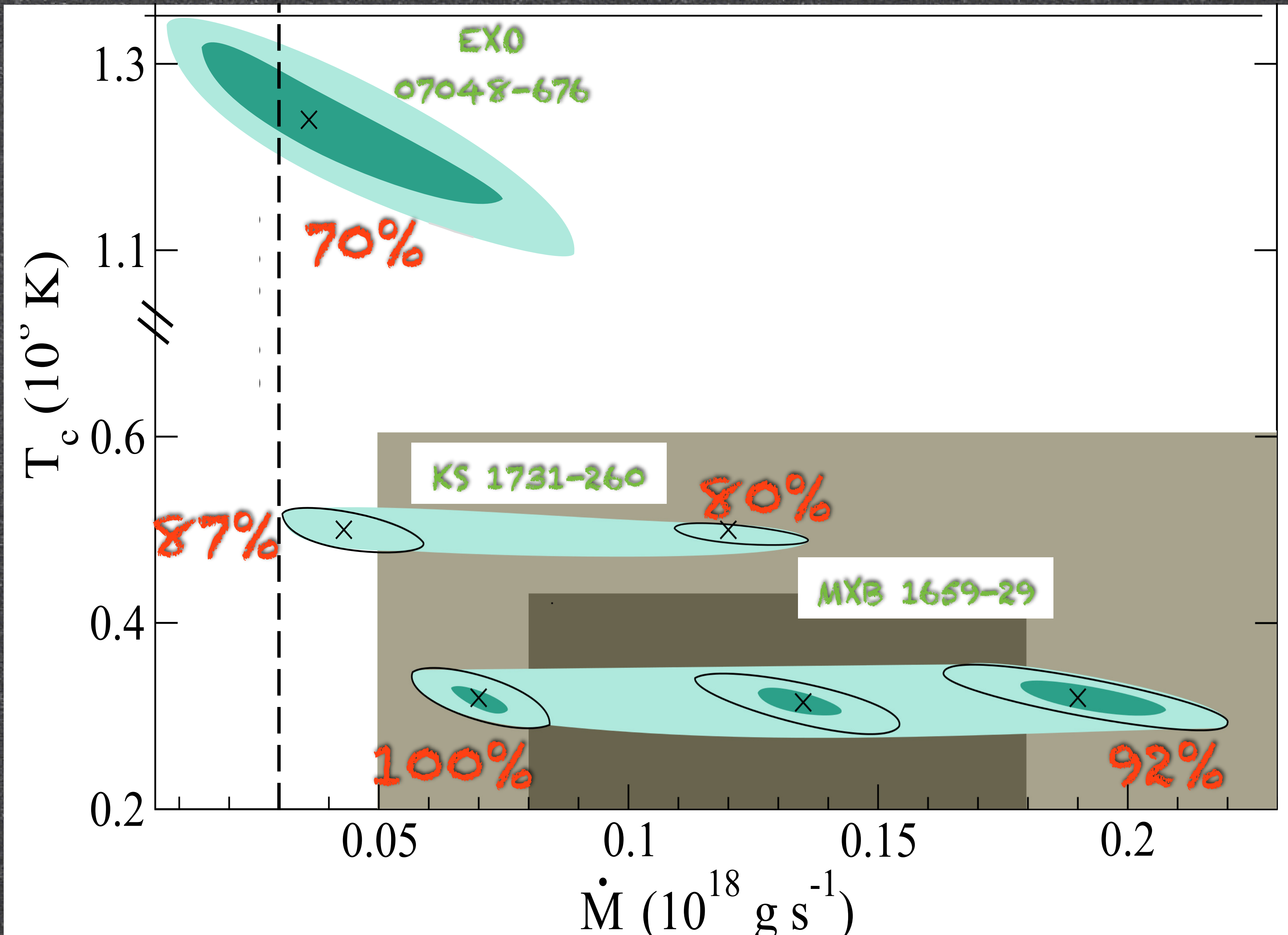

Crustal coolers

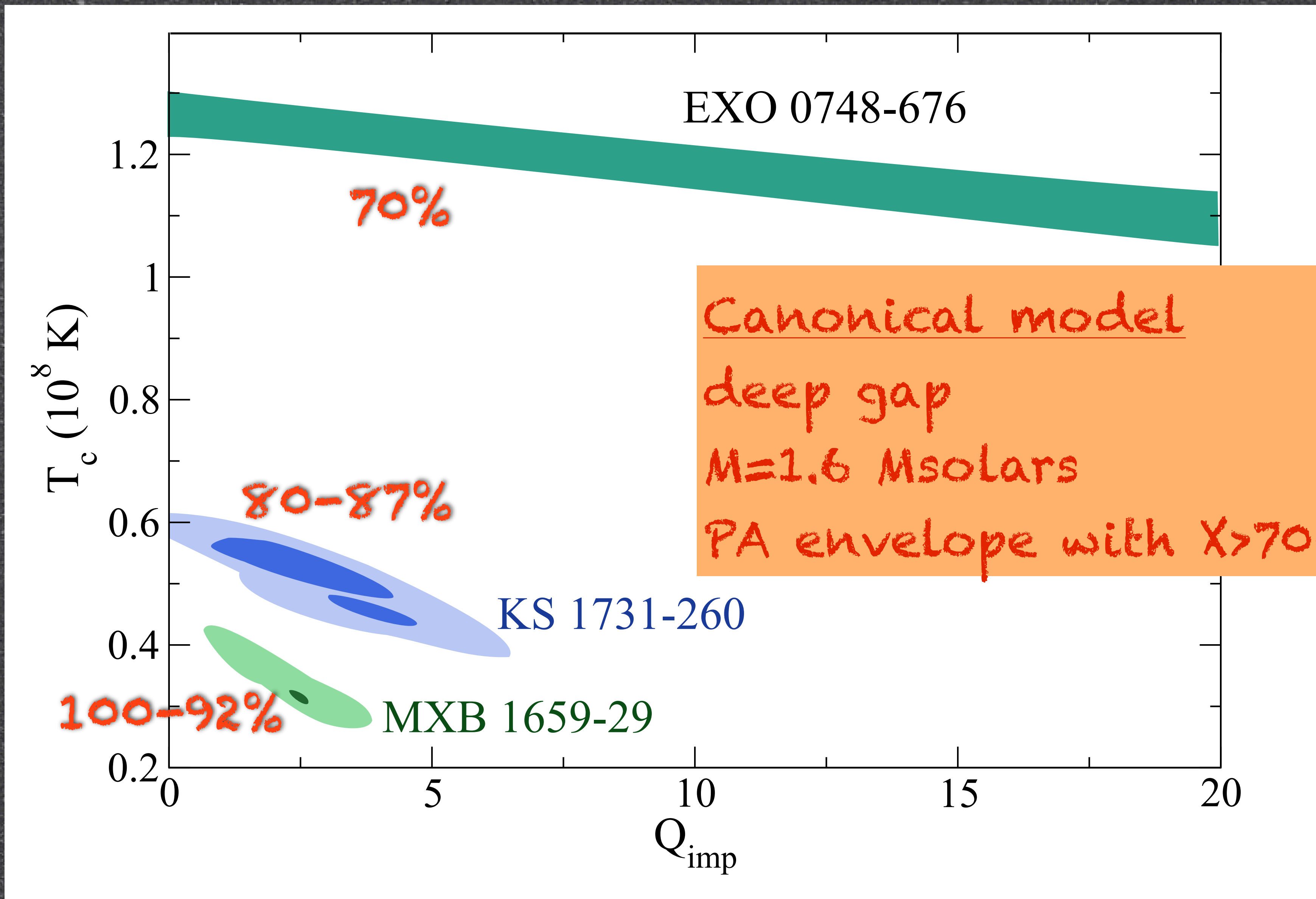

Canonical model

deep gap

M=1.6 Msolars

PA envelope with X>70-80 %

“Beyond” crustal cooling

XTE 1701-462: VARIABILITY

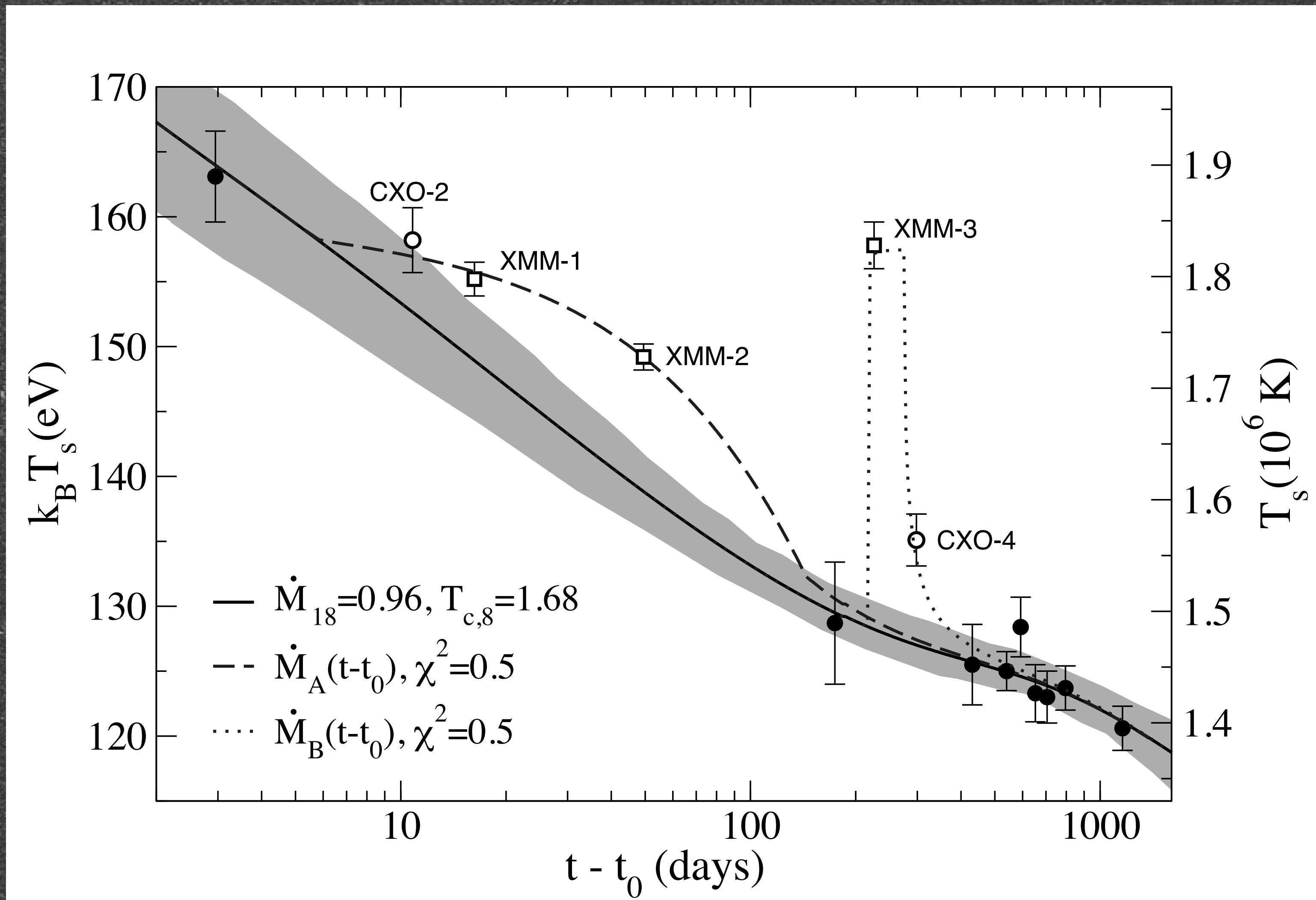

XTE 1701-462: VARIABILITY

residual accretion?

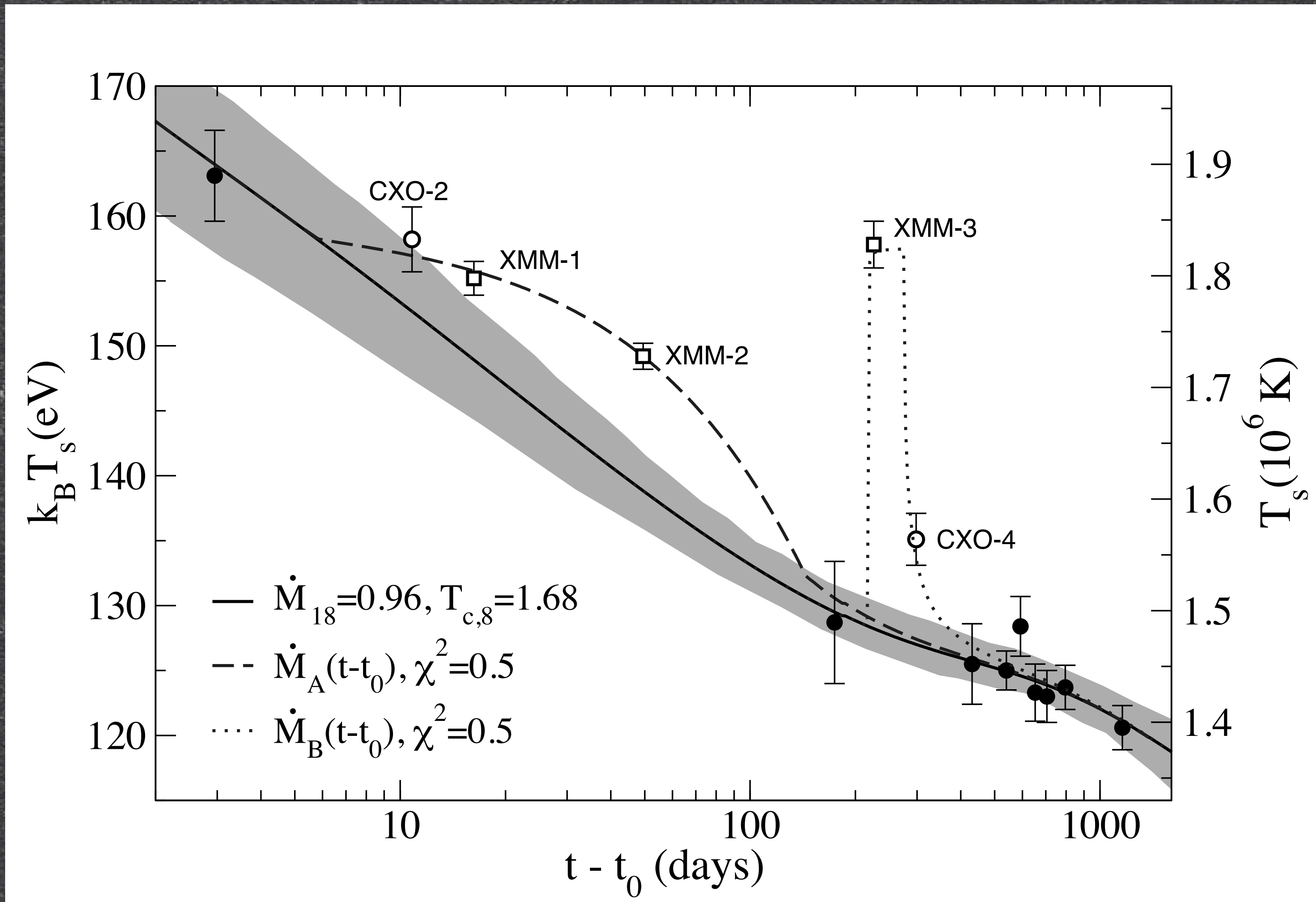

XTE 1701-462: VARIABILITY

residual accretion?

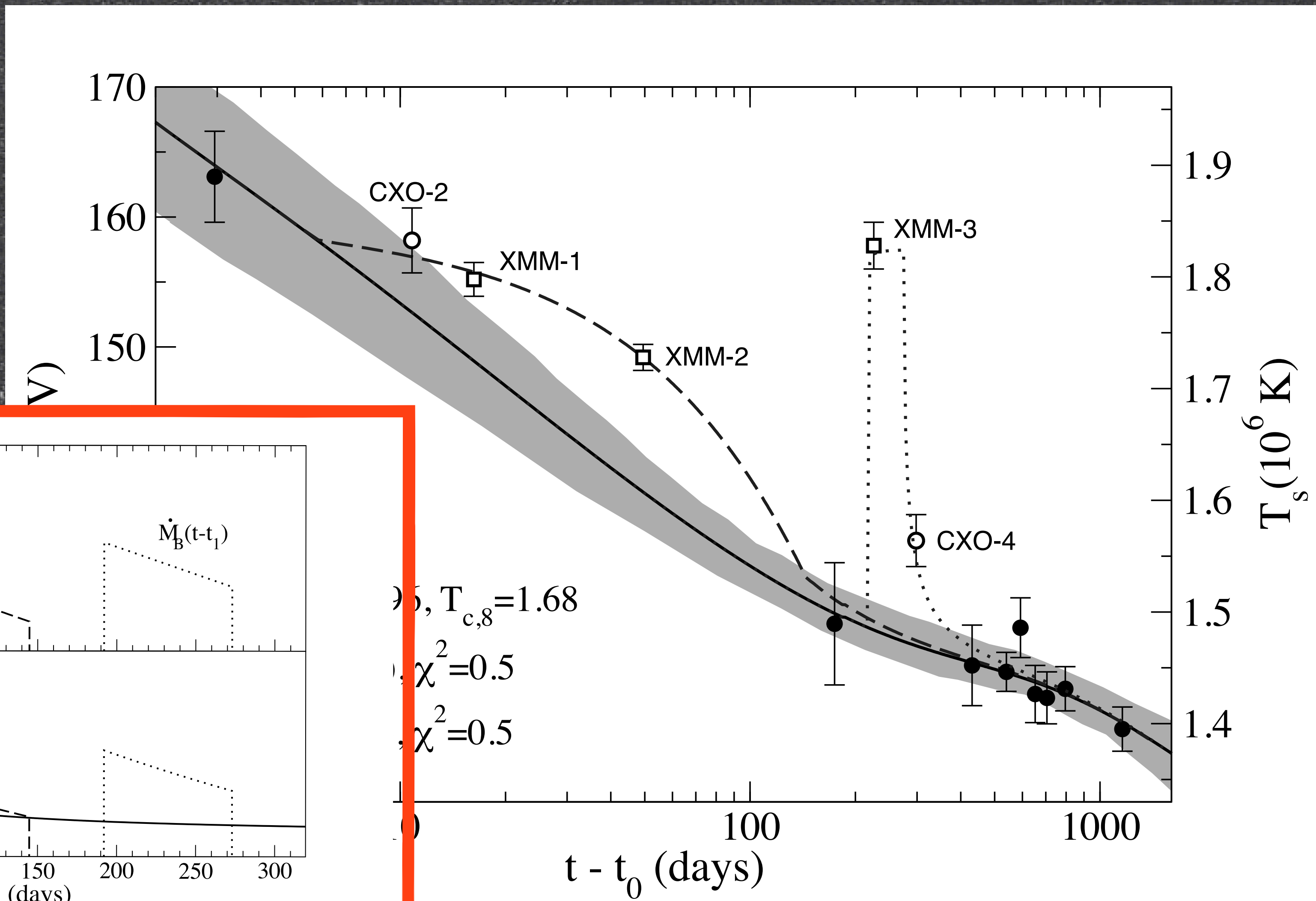

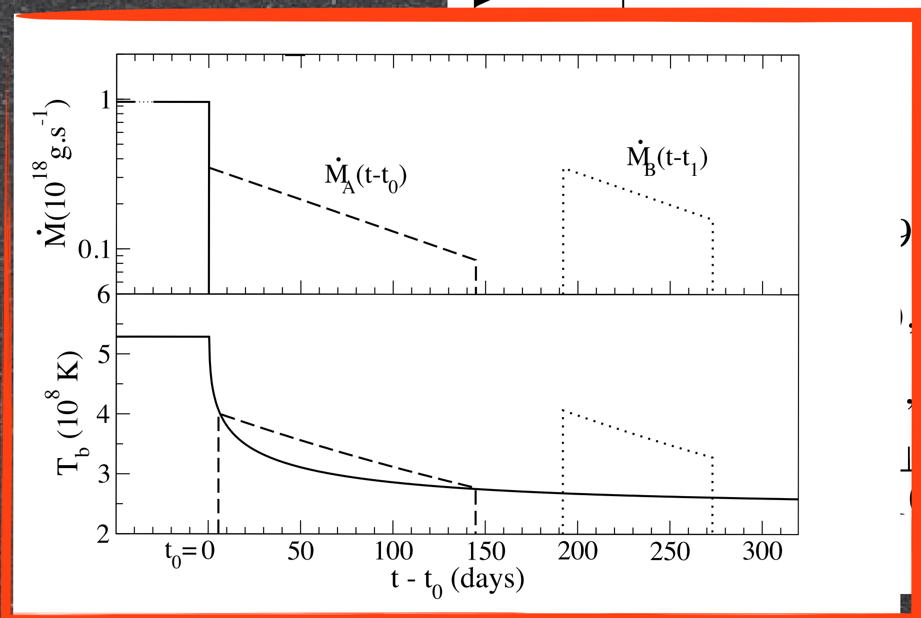

XTE 1701-462: VARIABILITY

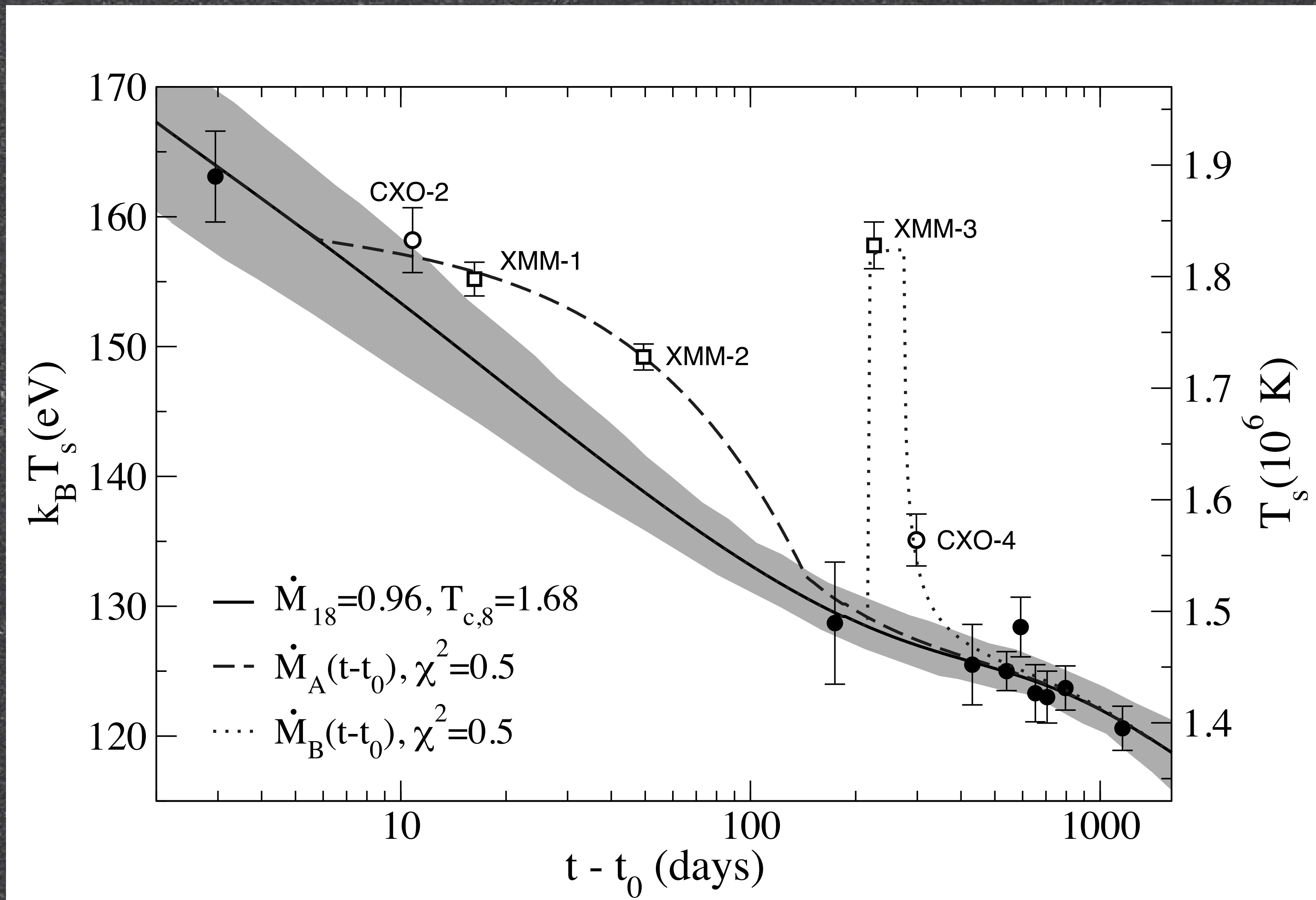

XTE 1701-462: VARIABILITY

other heat sources @ shallow depths?

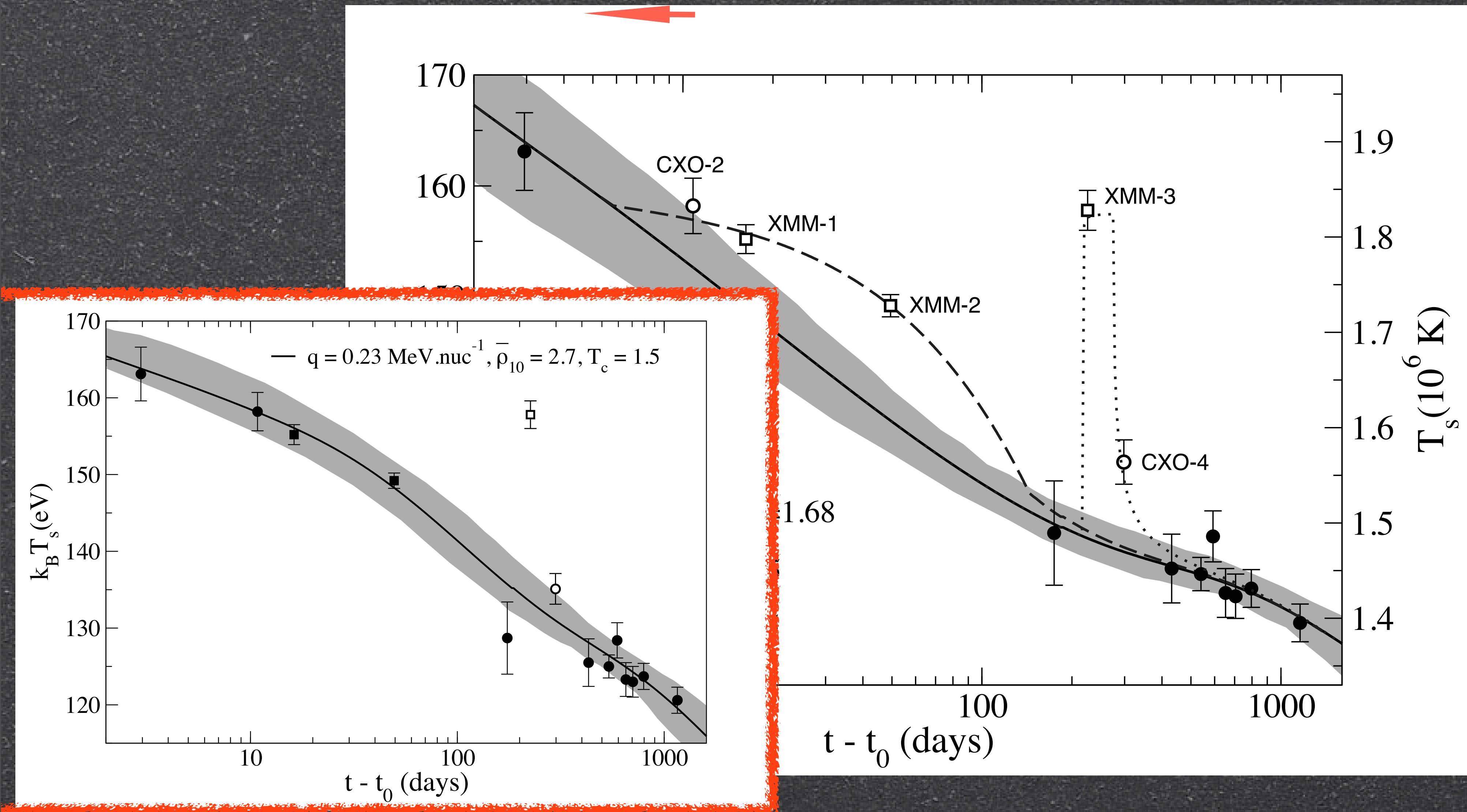

XTE 1701-462: VARIABILITY

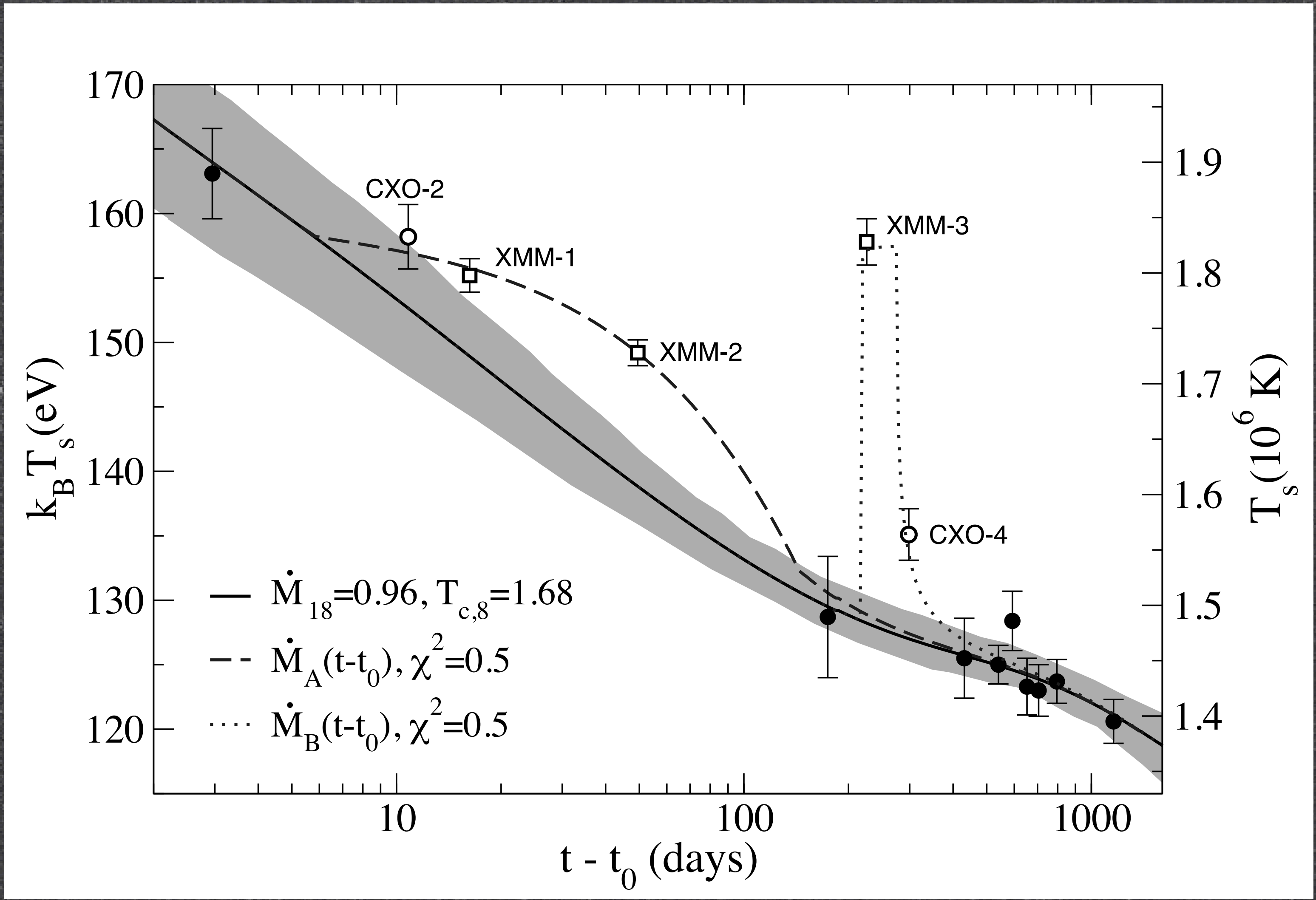

XTE 1701-462: VARIABILITY

thermal isolation inner/outer crust?

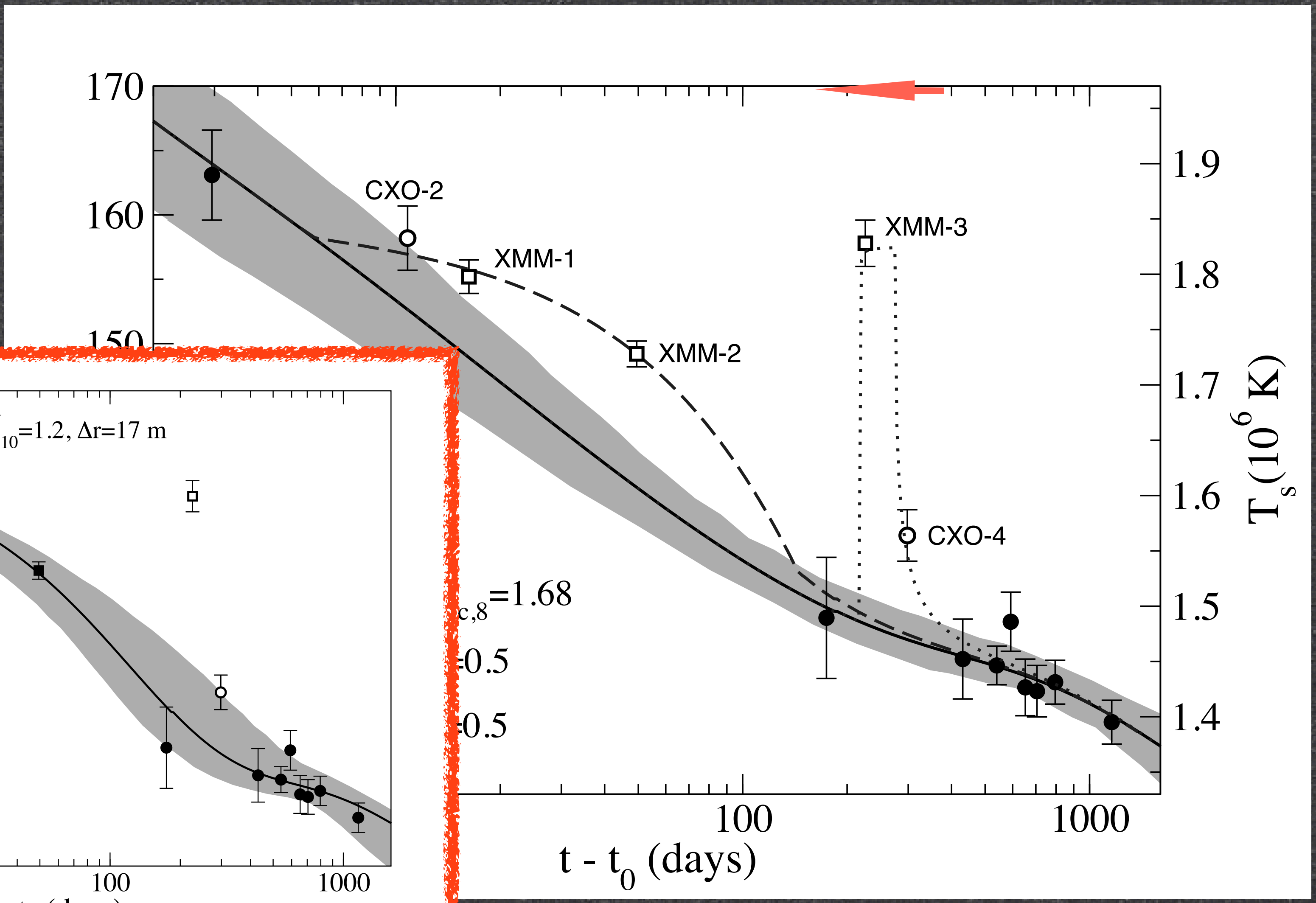

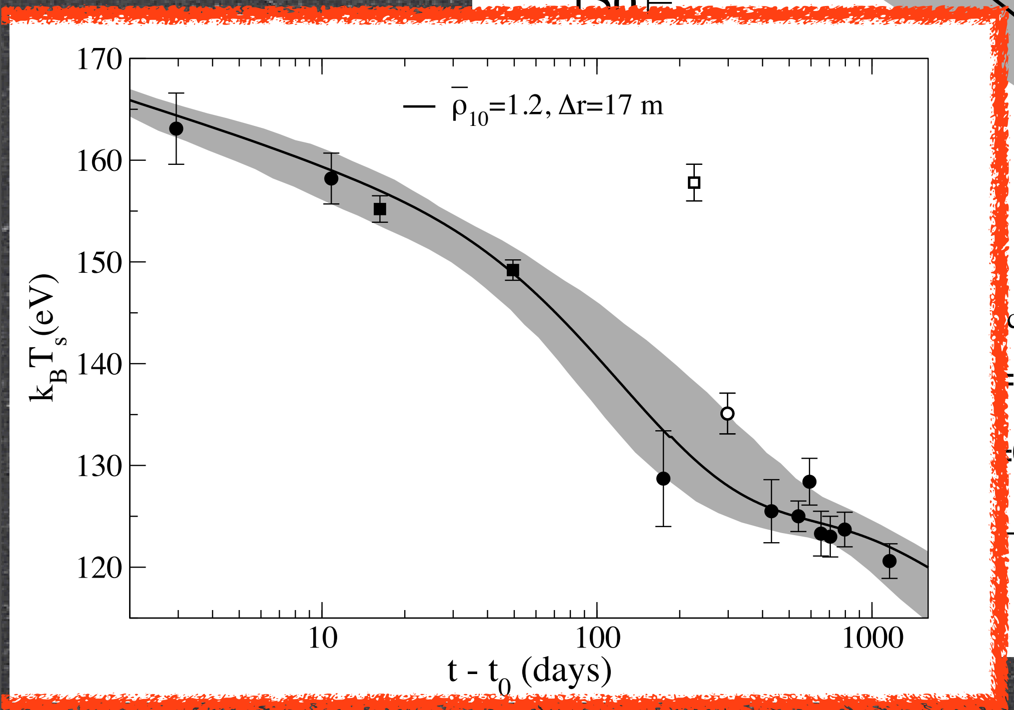

IG J17480-2446: accreting only for 2 months

with additional heat sources

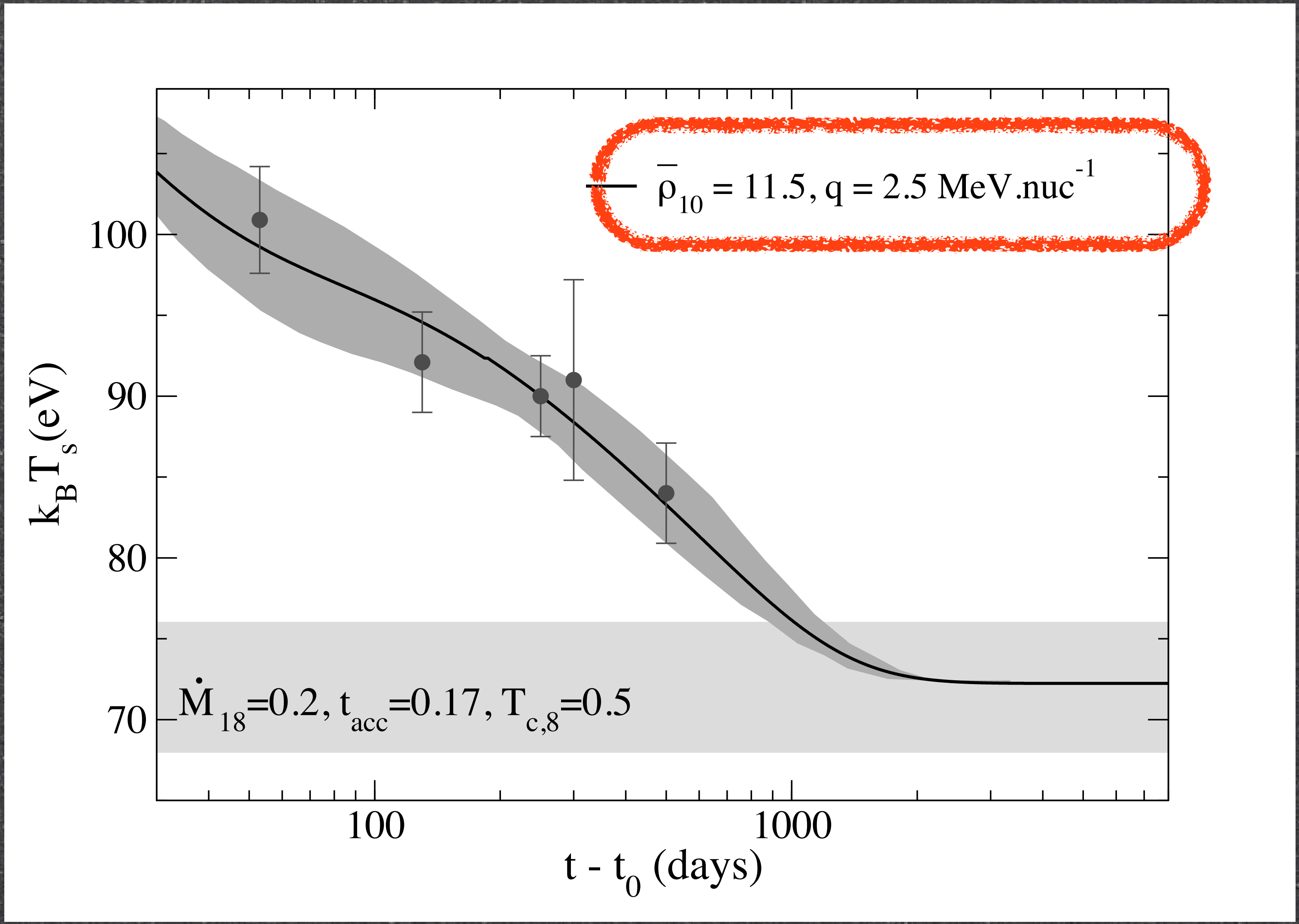

Additional heat sources in the outer crust?

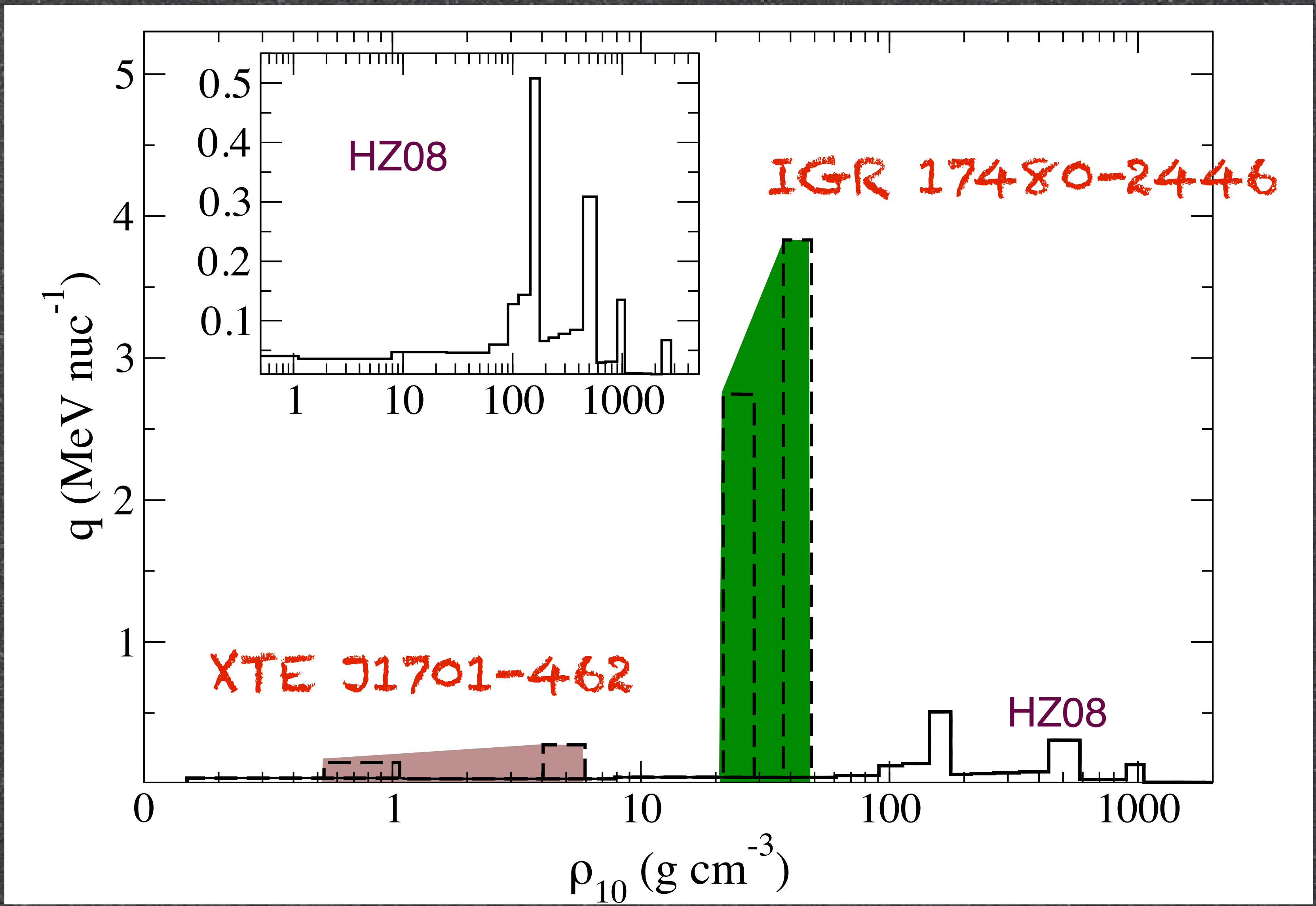

Summary

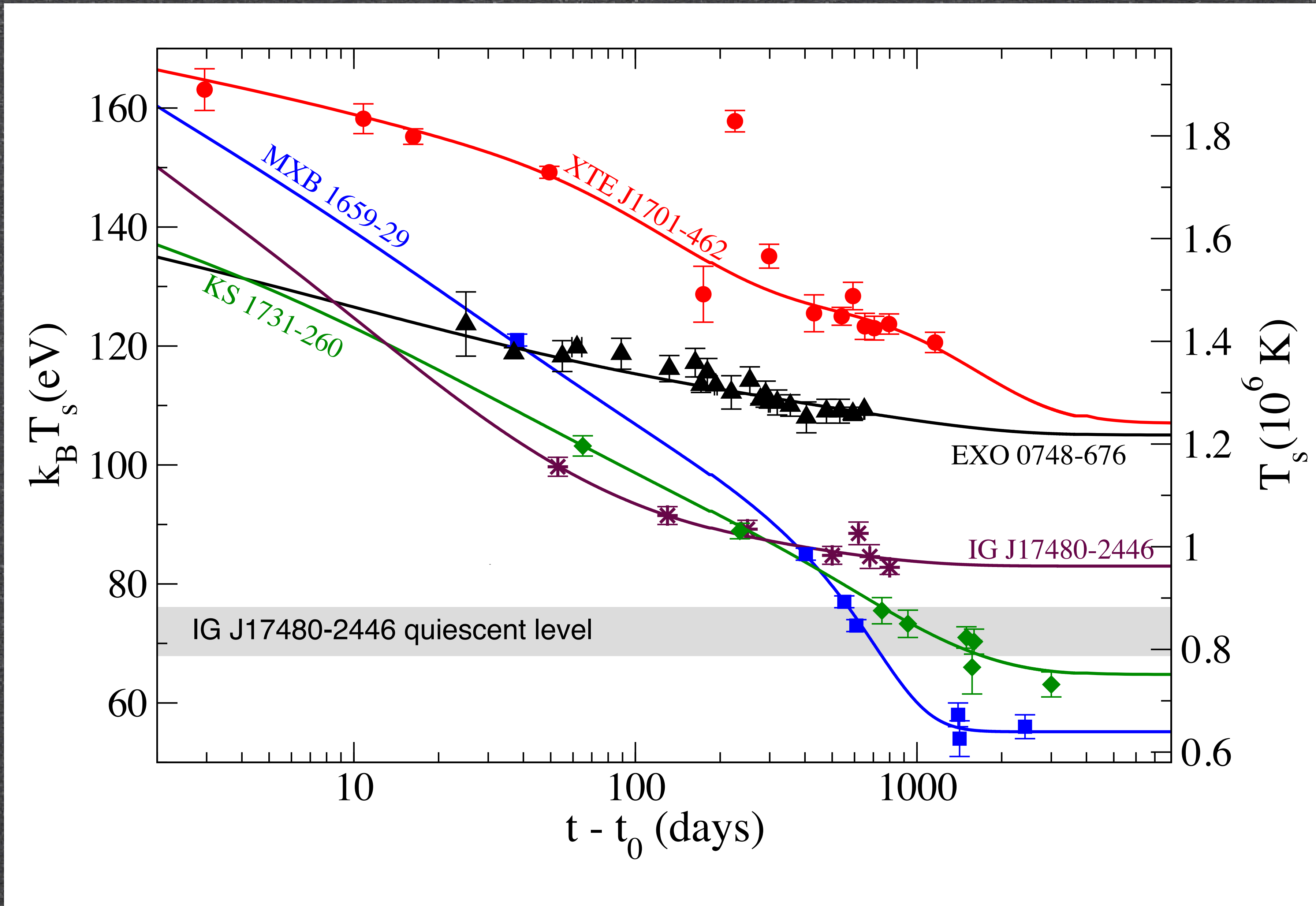

XTE J1701-462
MXB 1659-29
KS 1731-260
EXO 0748-676
IG J17480-2446
IG J17480-2446 quiescent level
$k_B T_s$ (eV)
T_s (10^6 K)
$t - t_0$ (days)

Conclusions

- Thermal evolution for the crust in quiescence for the five sources known

- Inclusion of the heated up envelope through the relation $T_b(\dot{M})$

  crust <-> envelope <-> outburst

- Constraints on
  - crust microphysics (Q_{imp}, SF n gap)
  - envelope composition (H/He fraction)

- Three sources are "deep crustal coolers"
- Two sources are beyond crustal cooling

  additional heat sources?, buried B, thermal wall?

THANKS !

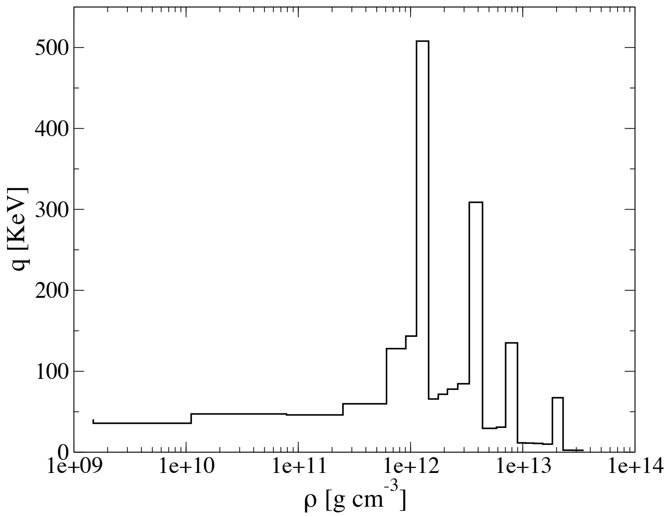

Fig3. Left panel: Heat sources in the crust. Right panel: Non-equilibrium processes in the crust of an accreting neutron stars assuming that the X-ray ashes consist of pure ^{56}Fe. P_j and ρ_j are pressure and density at which the reaction takes place. (Haensel & Zdunik 2008).

P (dyn cm^{-2})	ρ (g cm^{-3})	Process
7.23×10^{26}	1.49×10^{9}	$^{56}\mathrm{Fe} \rightarrow ^{56}\mathrm{Cr} - 2e^- + 2\nu_e$
9.57×10^{27}	1.11×10^{10}	$^{56}\mathrm{Cr} \rightarrow ^{56}\mathrm{Ti} - 2e^- + 2\nu_e$
1.15×10^{29}	7.85×10^{10}	$^{56}\mathrm{Ti} \rightarrow ^{56}\mathrm{Ca} - 2e^- + 2\nu_e$
4.75×10^{29}	2.50×10^{11}	$^{56}\mathrm{Ca} \rightarrow ^{56}\mathrm{Ar} - 2e^- + 2\nu_e$
1.36×10^{30}	6.11×10^{11}	$^{56}\mathrm{Ar} \rightarrow ^{52}\mathrm{S} + 4n - 2e^- + 2\nu_e$
1.980×10^{30}	9.075×10^{11}	$^{52}\mathrm{S} \rightarrow ^{46}\mathrm{Si} + 6n - 2e^- + 2\nu_e$
2.253×10^{30}	1.131×10^{12}	$^{46}\mathrm{Si} \rightarrow ^{40}\mathrm{Mg} + 6n - 2e^- + 2\nu_e$
2.637×10^{30}	1.455×10^{12}	$^{40}\mathrm{Mg} \rightarrow ^{34}\mathrm{Ne} + 6n - 2e^- + 2\nu_e$
		$^{34}\mathrm{Ne} + ^{34}\mathrm{Ne} \rightarrow ^{68}\mathrm{Ca}$
2.771×10^{30}	1.766×10^{12}	$^{68}\mathrm{Ca} \rightarrow ^{62}\mathrm{Ar} + 6n - 2e^- + 2\nu_e$
3.216×10^{30}	2.134×10^{12}	$^{62}\mathrm{Ar} \rightarrow ^{56}\mathrm{S} + 6n - 2e^- + 2\nu_e$
3.825×10^{30}	2.634×10^{12}	$^{56}\mathrm{S} \rightarrow ^{50}\mathrm{Si} + 6n - 2e^- + 2\nu_e$
4.699×10^{30}	3.338×10^{12}	$^{50}\mathrm{Si} \rightarrow ^{44}\mathrm{Mg} + 6n - 2e^- + 2\nu_e$
6.043×10^{30}	4.379×10^{12}	$^{44}\mathrm{Mg} \rightarrow ^{36}\mathrm{Ne} + 8n - 2e^- + 2\nu_e$
		$^{36}\mathrm{Ne} + ^{36}\mathrm{Ne} \rightarrow ^{72}\mathrm{Ca}$
		$^{72}\mathrm{Ca} \rightarrow ^{66}\mathrm{Ar} + 6n - 2e^- + 2\nu_e$
7.233×10^{30}	5.839×10^{12}	$^{66}\mathrm{Ar} \rightarrow ^{60}\mathrm{S} + 6n - 2e^- + 2\nu_e$
9.238×10^{30}	7.041×10^{12}	$^{60}\mathrm{S} \rightarrow ^{54}\mathrm{Si} + 6n - 2e^- + 2\nu_e$
1.228×10^{31}	8.980×10^{12}	$^{54}\mathrm{Si} \rightarrow ^{48}\mathrm{Mg} + 6n - 2e^- + 2\nu_e$
		$^{48}\mathrm{Mg} + ^{48}\mathrm{Mg} \rightarrow ^{96}\mathrm{Cr}$
		$^{96}\mathrm{Cr} \rightarrow ^{94}\mathrm{Cr} + 2n$
1.463×10^{31}	1.057×10^{13}	$^{94}\mathrm{Cr} \rightarrow ^{88}\mathrm{Ti} + 6n - 2e^- + 2\nu_e$
1.816×10^{31}	1.254×10^{13}	$^{88}\mathrm{Ti} \rightarrow ^{82}\mathrm{Ca} + 6n - 2e^- + 2\nu_e$
2.304×10^{31}	1.506×10^{13}	$^{82}\mathrm{Ca} \rightarrow ^{76}\mathrm{Ar} + 6n - 2e^- + 2\nu_e$
2.998×10^{31}	1.838×10^{13}	$^{76}\mathrm{Ar} \rightarrow ^{70}\mathrm{S} + 6n - 2e^- + 2\nu_e$
4.028×10^{31}	2.287×10^{13}	$^{70}\mathrm{S} \rightarrow ^{64}\mathrm{Si} + 6n - 2e^- + 2\nu_e$
		$^{64}\mathrm{Si} + ^{64}\mathrm{Si} \rightarrow ^{128}\mathrm{Ni}$
		$^{128}\mathrm{Ni} \rightarrow ^{126}\mathrm{Ni} + 2n$
5.278×10^{31}	2.784×10^{13}	$^{126}\mathrm{Ni} \rightarrow ^{124}\mathrm{Fe} + 2n - 2e^- + 2\nu_e$
7.311×10^{31}	3.493×10^{13}	$^{124}\mathrm{Fe} \rightarrow ^{122}\mathrm{Cr} + 2n - 2e^- + 2\nu_e$

Accreted crust composition

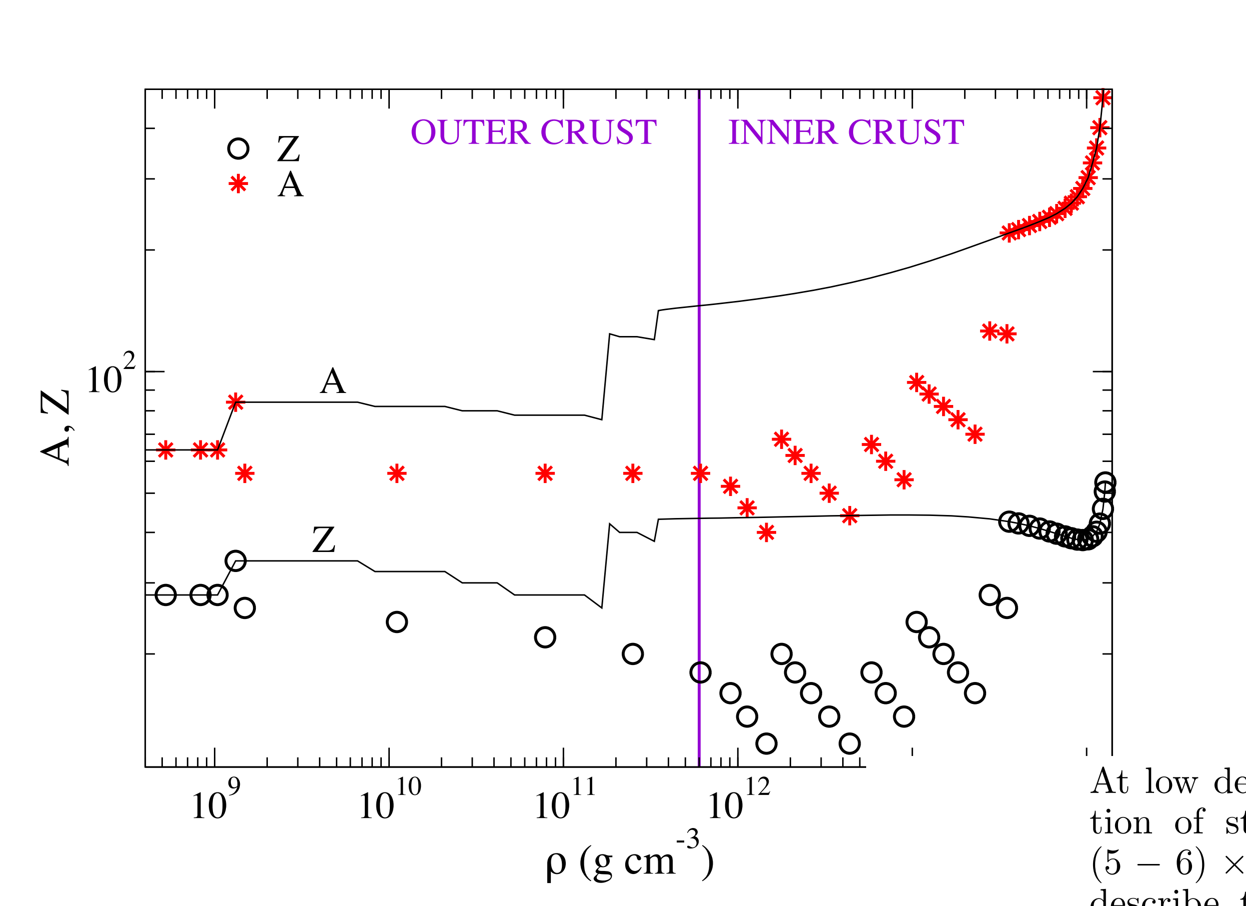

At low density we use the BBP Baym et al. (1971) equation of state. The crust-envelope interface is placed at $(5-6)\times10^8\,\mathrm{g\,cm^3}$ and we continue using BBP EoS to describe the crust up to the density $1.49\times10^9\,\mathrm{g\,cm^{-3}}$. To take into account the effects of the accretion in the crust composition, we use the EoS presented in HZ08 in the range $\rho=(1.49\times10^9-3.5\times10^{13})\,\mathrm{g\,cm^{-3}}$. This is a BBP-like EoS but modified by non-equilibrium nuclear reactions in the crust (see next Section). To describe the very high density region in the inner crust and the core we use Douchin & Haensel (2001), a Skyrme-type EoS which considers a nucleon-nucleon SLy effective interaction. For this chosen EoS the crust-core interface is at $0.5\,\rho_0$, where $\rho_0=2.8\times10^{14}\,\mathrm{g\,cm^{-3}}$ is the nuclear saturation density.

Accreted crust composition

from Haensel & Zdunik 2008

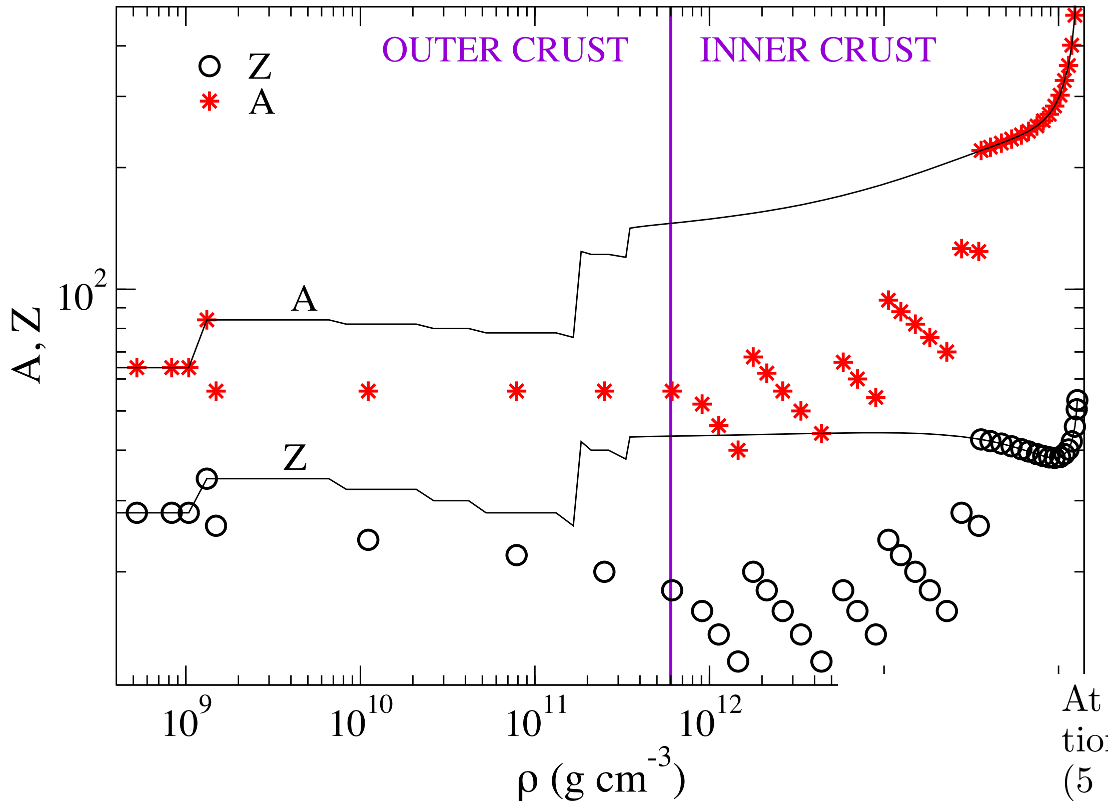

At low density we use the BBP Baym et al. (1971) equation of state. The crust-envelope interface is placed at $(5-6) \times 10^8\,\mathrm{g\,cm^3}$ and we continue using BBP EoS to describe the crust up to the density $1.49 \times 10^9\,\mathrm{g\,cm^{-3}}$. To take into account the effects of the accretion in the crust composition, we use the EoS presented in HZ08 in the range $\rho = (1.49 \times 10^9 - 3.5 \times 10^{13})\,\mathrm{g\,cm^{-3}}$. This is a BBP-like EoS but modified by non-equilibrium nuclear reactions in the crust (see next Section). To describe the very high density region in the inner crust and the core we use Douchin & Haensel (2001), a Skyrme-type EoS which considers a nucleon-nucleon SLy effective interaction. For this chosen EoS the crust-core interface is at $0.5\,\rho_0$, where $\rho_0 = 2.8 \times 10^{14}\,\mathrm{g\,cm^{-3}}$ is the nuclear saturation density.

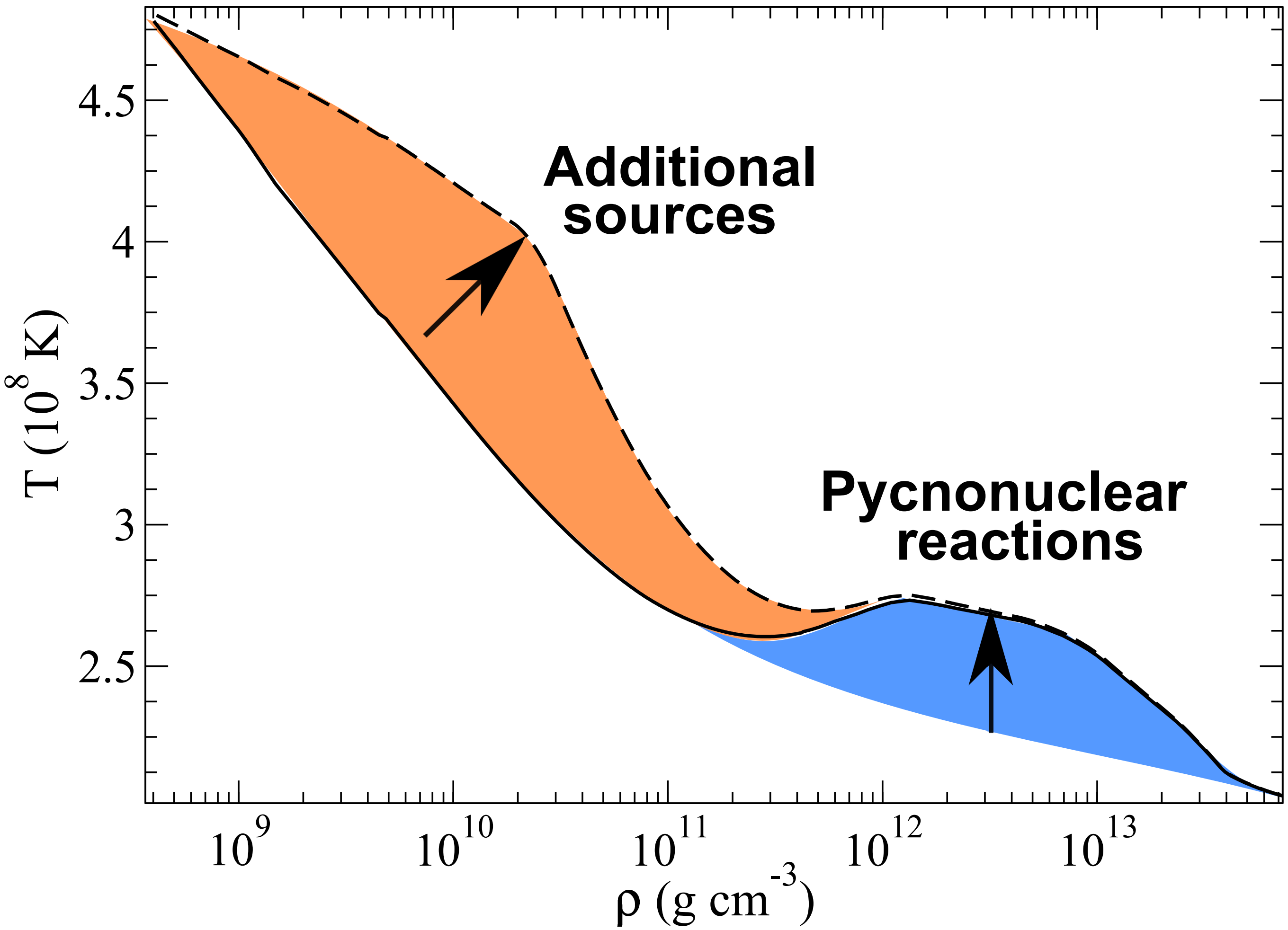

Fig. 17. Heat sources that influence on the initial thermal profile.

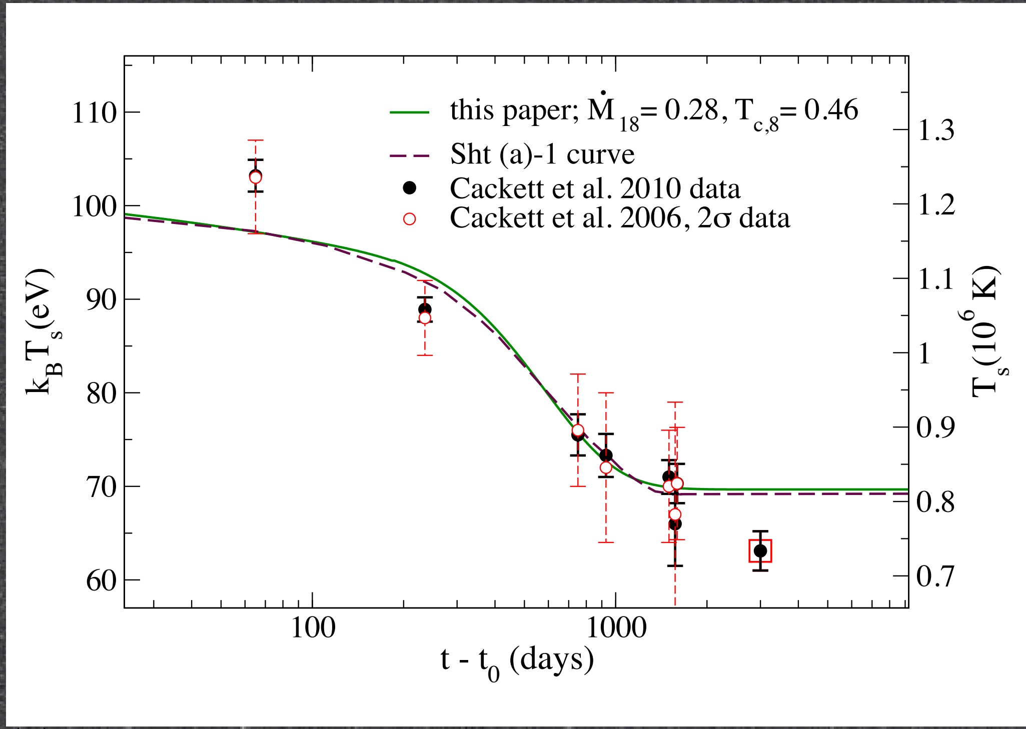

(a) Solid line is our curve with $Q_{\rm imp} = 2$. Dashed curve is from Sht07.

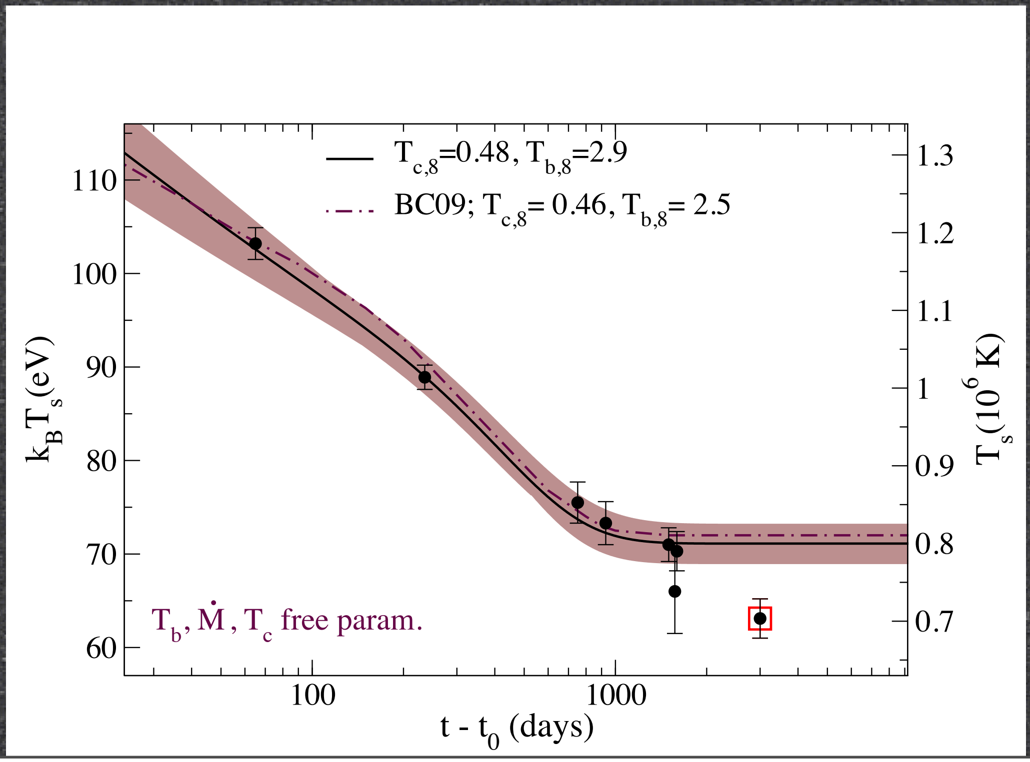

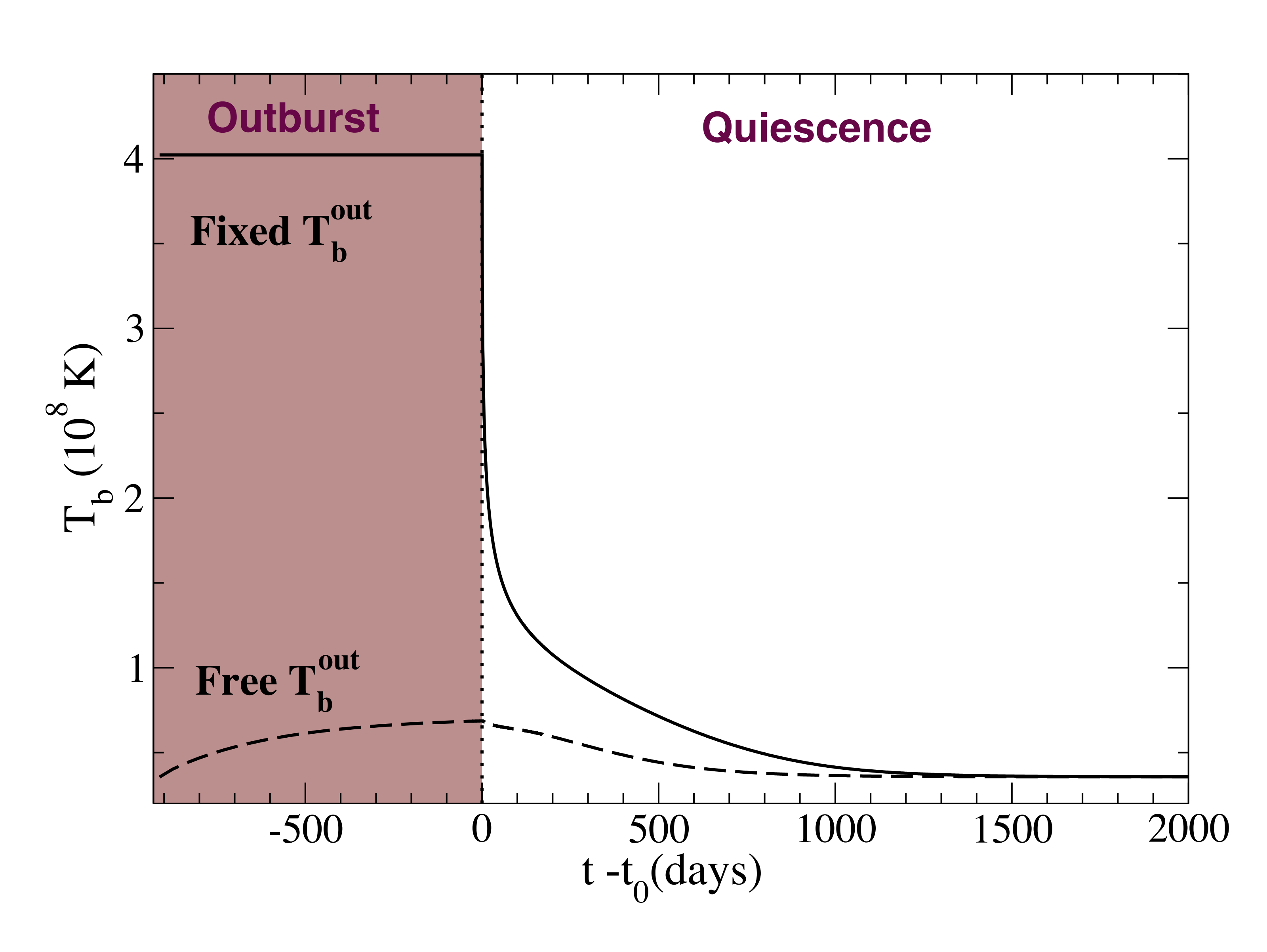

(a) Temperatures at the crust-envelope interface

The initial thermal profile

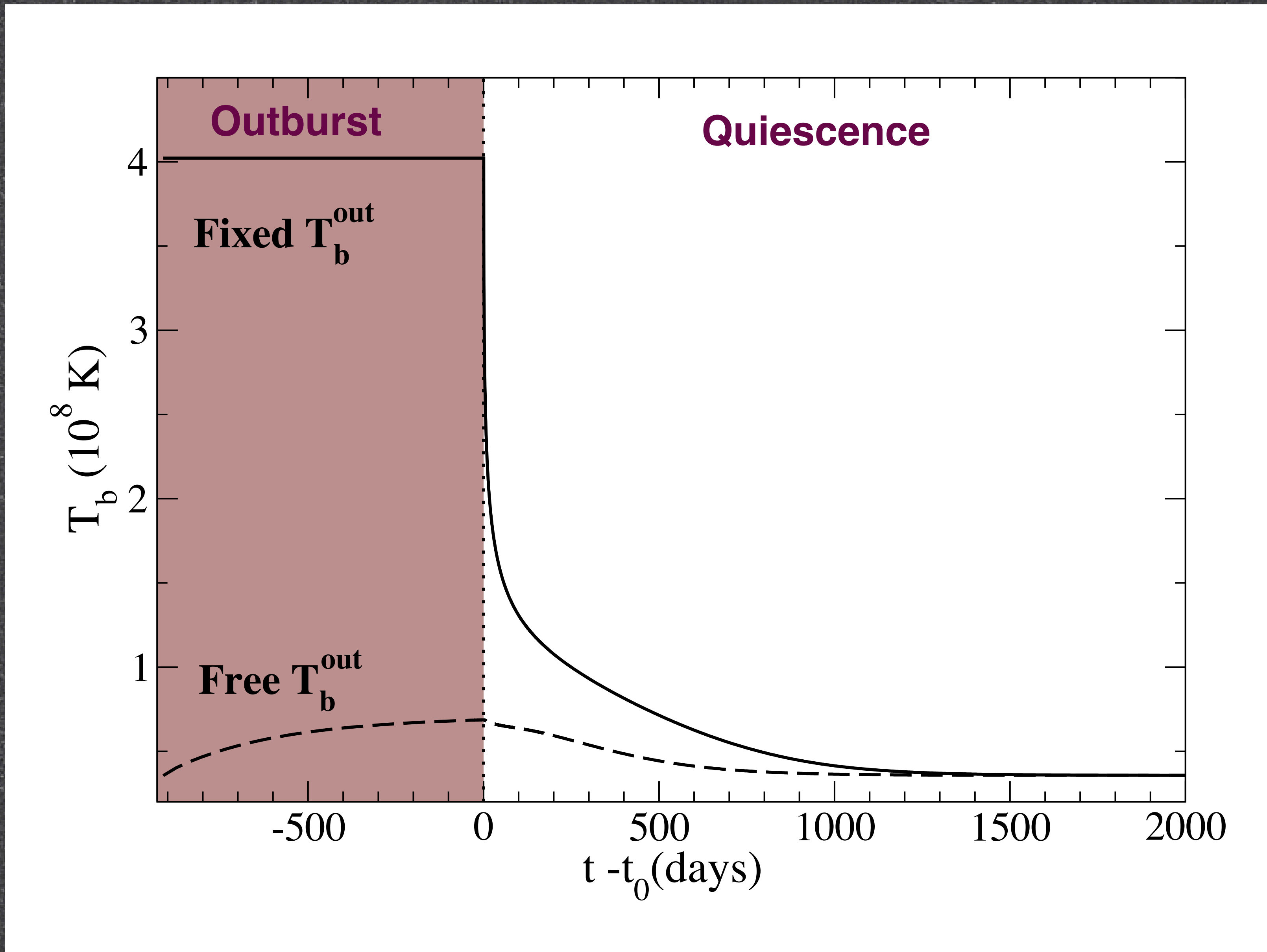

(a) Temperatures at the crust-envelope interface heating flux as: $F = E_{\rm nuc}\dot{m}$,

Hot CNO cycle

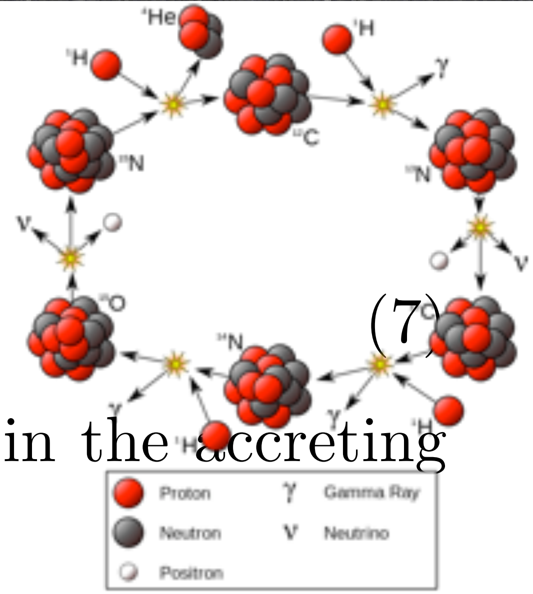

$$\epsilon_{\rm h} = 5.8 \times 10^{15} Z_{\rm CNO}\ {\rm erg\,g^{-1}\,s^{-1}}, \tag{7}$$

where $Z_{\rm CNO}$ is the mass fraction of CNO in the accreting matter.

3 alpha

$$\epsilon_{3\alpha} = 5.3 \times 10^{21} \rho_5^2\, Y^3\, \frac{\exp(-44/T_8)}{T_8^3}\ {\rm erg\,g^{-1}\,s^{-1}}, \tag{8}$$

$$\boxed{\begin{aligned} E_{\rm h}\,\dot{m}\,X &= \epsilon_h\, y_{\rm H} \quad \text{for} \quad \text{H} \\ E_{3\alpha}\,\dot{m}\,Y &= \epsilon_{3\alpha}\, y_{\rm He} \quad \text{for} \quad \text{He} \end{aligned} \quad (9) \\ \text{where } E_{\rm h} = 6.4\times 10^{18}{\rm erg\,g^{-1}} \text{ and } E_{3\alpha} = 5.84\times 10^{17}{\rm erg\,g^{-1}}.}$$

Assuming Thomson scattering

$$T_{\rm ign,He} \sim \frac{1.83 \times 10^8 {\rm K}}{\kappa^{1/10} Y^{3/10} (\mu g_{14} y_8^2)^{1/5}} \tag{10}$$